

AN INVESTIGATION TO IMPROVE SELENODETIC
CONTROL THROUGH SURFACE AND ORBITAL
LUNAR PHOTOGRAPHY

Harry Jauncey Sweet

AN INVESTIGATION TO IMPROVE SELENODETIC CONTROL
THROUGH SURFACE AND ORBITAL LUNAR PHOTOGRAPHY

A Thesis

Presented in Partial Fulfillment of the Requirements
for the Degree Master of Science

by

Harry Jauncey Sweet III, B. S.

The Ohio State University
1970

ACKNOWLEDGEMENT

Appreciation for the invaluable aid in programming and programming assistance of Mr. Dewey Watts and the provision of lunar photographic materials by the Mapping Sciences Laboratory, Manned Spacecraft Center Houston, Texas and its Data Bank, particularly, is hereby acknowledged. Gratitude is further extended to The Ohio State University Computer Center and National Science Foundation for services rendered as well as to the United States Navy for making advanced study available to me.

TABLE OF CONTENTS

	<u>Page</u>
ACKNOWLEDGEMENT	i i
TABLE OF CONTENTS	iii
1. INTRODUCTION	1
2. ABSTRACT	2
3. HISTORICAL REVIEW	3
4. EXPERIMENTATION	10
4.1 Real Data Experiment	10
4.1.1 Preliminary	10
4.1.2 Materials	10
4.1.3 Procedure	11
4.1.4 Real Data Results	18
4.2 Idealized Data Experiment	19
4.2.1 Procedure	19
4.2.2 Idealized Data Results	22
5. CONCLUSIONS	43
6. RECOMMENDATIONS	45
6.1 Concept	45
6.2 Presupposition	45
6.3 Equipment	46
6.4 Procedure	46
BIBLIOGRAPHY	51
APPENDICES	55
I COMCORDCON	55
II BLOCK TRIANGULATION PROGRAM	67

1. INTRODUCTION

The purpose of this paper is to explore the use of lunar surface photography in order to achieve the photogrammetric transfer of available selenographic coordinates from future lunar landing sites to neighboring, photoidentifiable features. It can be implied from the procedures developed that overhead photography, were it available, could be utilized and would provide a material strengthening of the total solution. By the methodic selection of features and confirmation that they can in reality be identified from orbital photography, a modest selenodetic control system can be expanded into a net that could ultimately control all future, manned or unmanned, orbital photographic missions.

2. ABSTRACT

For centuries man has scrutinized the moon in one manner or another and postulated theories concerning its size, shape, origin, and other general characteristics. With the passage of time and the improvement of equipment and observation techniques the desire for more explicit information concerning earth's nearest celestial neighbor has become acute. In fact, as the moment approached when man would actually set foot on the lunar surface, the need for such information became vital. The following historical review briefly outlines man's effort to improve his knowledge in one of the pertinent regions of selenodesy — selenodetic control.

The remainder of this paper explores a method of improving the existing selenodetic control by employing available lunar surface photography supplemented by that obtained from lunar orbit. Following the results of this experiment an ideal model is submitted. The unknowns associated with this model are perturbed within realistic limits by a random number generation program. This provides a theoretical indication of the accuracy that could be anticipated assuming there is reasonable adherence to the suggested procedures.

Finally, conclusions are drawn and reasonable recommendations are offered to improve selenodetic control by the photogrammetric transfer of known or assumed, local or astronomic coordinates of a lunar landing site to neighboring features that may be photoidentified from orbital photographs.

3. HISTORICAL REVIEW

For decades in the past to the present day the task of surveying the moon has engaged the efforts of many astronomers. In early 1959 the launching of LUNIK I by Russia, and subsequently, POINEER IV by the United States: "...opened the first modern, post telescopic phase of lunar exploration." or, at least, introduced a tantalizing new dimension [30].

During the some seventy years prior to the launching of the first lunar space probes the establishment of selenodetic control was founded on direct astronomic angular observations and indirect angular observations through astronomic photography. Essentially, it was based on heliometric observations which consist of measurements of position angles and angular distances between a reference point on the lunar surface (Mösting A is the fundamental point) and the lunar limb. Observations at mean libration permit a best-fit circle of the lunar disc to be established. The center of this circle is defined as the projection of the origin of the coordinate system (the dynamic or mass center of the moon) upon the lunar surface and its radius to be the mean radius of the moon. Thus, the center of figure is equated to the center of mass and in the adjustment of the heliometric observations this injects the so-called center of figure bias. The adjustment provides corrected values of physical lunar libration parameters and the coordinates of the reference point as well as the mean radius of the moon [26].

The heliometer was first developed by Bouger in 1748 and later modified by Dollond. It consists of a refractor telescope with two semi-lenses which may form a single, superimposed image of two object points at the principle focus. The angular distance between the two object points formed on the focus is equal to the distance between the centers of the semi-lenses when one slides parallel to a line of section upon the other [24]. It was used to measure the diameter of the moon at the end of the 18th century by Lalande

and by Bessel in 1839 to investigate lunar physical librations. It was Bessel that developed the procedures for measurement that remain basically intact today.

Heliometric observations are limited by the resolving power imposed by their relatively small apertures (4-7 inches). The Rayleigh criterion:

$$\theta = 1.22 \frac{\lambda}{D}$$

θ = minimum angle resolved in minutes

λ = wavelength of light

D = diameter of objective lens

theoretically indicates that a six inch aperture provides a minimum resolution of 0.75 arc seconds or well over a kilometer on the moon's surface. A further limitation is based on atmospheric refractivity [20].

Selenodetic control systems derived from earth-based lunar photography generally rely heavily on heliometric observations. The reduction of these observations provide the libration parameters (f, l) and the coordinates of fundamental points. These reference points provide the orientation and scale of the photographs from which the plate constants are determined.

A German astronomer, Franz, established the original eight fundamental points in the early 1900's. Through the use of five plates from Lick Observatory he expanded these to a system of 150 points. By 1958, an Austrian astronomer, Schrutka-Rechtenstamm, published a revision of the moon libration theory and a recomputation of Franz's 150 points. This system is considered the best available and has served as the basis for later, more densified systems [26]. Yet the S-R system and others comparable to it reflect the inaccuracies inherent in the original heliometric observations as well as the additional inaccuracies associated with the earth-based photographic process.

Two American government agencies have undertaken densification of

lunar control. The Army Map Service (now, Army Topographic Command) published AMS-64 consisting of 256 points. This agency utilized the fundamental points from the IAU Catalogue of Blagg and Muller and plates from the Lick Observatory [8]. In 1966, AMS published the GROUP NASA system of 484 points utilizing control points determined by Saunder, Franz, and Konig [18]. The Aeronautical Chart and Information Center of the U. S. Air Force published another independent system of 196 points in 1965. ACIC selected Control from the S-R system and plates from the Pic du Midi Observatory in France and the U. S. Navy Astrometric Reflector in Arizona [23]. There were large differences between the systems of the two agencies in planimetry (several kilometers) and height. This was emphasized during the RANGER probes to the moon when elevation differences of approximately 2.5 kilometers between the AMS/ACIC systems and the trajectory computations were noted. Nevertheless, the systems were combined to form the Selenodetic Control System, DOD-66, of 734 points [26][19].

Two modern photographic methods are independent of control established through heliometric observations and appear to be rather promising. The Lunar and Planetary Laboratory at the University of Arizona employs a procedure using star trailed photography that was designed by Arthur [26]. Perhaps more significant is a procedure contributed by Kopal of the University of Manchester. Moutsoulas describes it as photographing a stellar field that is at the same declination and hour angle that the moon will attain at a later time. When the moon reaches the proper position, the plate is reexposed. Providing no excessive temperature changes take place during the period the telescope is stationary, the star field provides the plate orientation and scale; and the constants can be used for reduction of points on the lunar surface [24]. Kopal states that the achieved accuracy is sufficient to determine the physical librations of the moon [22].

Extensive, extraterrestrial photography was inaugurated with the launching of the Lunar Orbiter Satellites during the period August 1966 and

August 1967. The mission of the first three Orbiters was primarily designed for the selection of primary and secondary landing sites for subsequent Apollo missions. Orbiter IV and V were tasked to perform a broad, systematic survey of scientifically interesting features on the lunar surface.

All Orbiter photographic subsystems contained a medium resolution lens (focal length 80 mm) and a high resolution lens (focal length 610 mm). Neither was of photogrammetric quality. Calibration of the system, in general, included determination of the calibrated focal length, radial and tangential distortion, the principle point of autocollimation and the camera format reference system with respect to sawtooth fiducials and a preexposed reseau system on the film (Lunar Orbiter I lacked these reseau marks). Additional calibration was required to establish the effect of an image motion compensation system.

In operation, the film would be clamped to the platen, and the platen would move in proportion to ground speed while the shutter was open. The film was then processed by a BIMAT system which developed, fixed, and dried it. The negative was then scanned by a line scan tube in small increments (2.67 mm). This signal was electronically processed for transmission to earth via the spacecrafts' telemetry subsystem as a composite video signal. The ground reconstruction electronics system received the video signal and fed it to a kinescope tube from which it was copied on 35 mm television recording film. A reassembly printer utilized this record to orient and project the framelets on aerographic duplicating film to produce the finished product.

The photography collected from this series eliminated several significant limitations attached to earth based photography; namely, the distortions associated with atmospheric refractivity and insufficient scale for effective resolution. Further, it provided a greatly improved geometry. However, other disadvantages inherent in the total system design requirements introduced distortions into the photography and uncertainties into the reduction procedures. Broadly, the distortions were associated with on board photographic processing, space transmission of the video signal, and ultimate reconstruction of the photo.

Reduction uncertainties included the film distortion, but additionally, was largely dependent upon photo support data which defined spacecraft location and attitude at time of exposure. These were functions of the orbit determination program with its associated uncertainties.

Nevertheless, despite the fundamental inaccuracies, ACIC evaluated the feasibility of establishing a lunar geodetic system from Lunar Orbiter photography and arrived at positive conclusions [3]. One result was, A Positional Reference System of Lunar Features Determined From Lunar Orbiter Photography. Although the original feasibility study encompassed only the Lunar Orbiter IV Mission with its polar orbit and extensive coverage, it was found that the medium resolution photography was of particularly poor quality in detail except near the terminator. The remainder was either highly over or under exposed. All photography possessed significant errors in timing, exposure orientation, and spacecraft positioning[3]. As a result, photography from all Lunar Orbiter missions was utilized in order to achieve the desired coverage. However, Lunar Orbiter I photos which lacked a pre-exposed reseau grid on the film were employed only when necessary to fill in specified areas. The method used, broadly, for this control system is best described by the author:

"The method consists of computing perspective projections [23] based upon the orbital data for a series of photographs that are linked together by common coverage. Starting on the nearside [of the moon], the projections were positioned to agree with the coordinates of features determined from telescope photography. [The ACIC net of 196 control points, [23]]. The link was continued around the moon by extending the coordinates of common features from one photograph to the next. A meridional arc and an equatorial arc were completed and joined in the vicinity of the equator and the 180th meridian [27].

This net produced (considering the extent of the net and lack of farside control) reasonable estimated accuracies of 1-5, 5-10, and 10-15 kilometers, depending on the particular area cited [27]. This was achieved despite the facts that control was provided only on the nearside in a coordinate system based on center of figure, and the photography was of variable quality with all the errors associated with its on board processing and electronic transmission. Further, the exterior elements of camera orientation were determined from spacecraft telemetry with the associated orbit determination uncertainties and a coordinate system originating at the center of mass.

A current control net in the process of being established by the Mapping Sciences Branch of the Manned Spacecraft Center, Houston, Texas, is in the imminent stages of completion. This net is based on medium and high resolution photography acquired solely by Lunar Orbiter IV. It covers a rather extensive area between $\pm 20^\circ$ latitude and 60° west longitude to 45° east longitude with the greatest concentration of control in the Apollo landing zone of $\pm 5^\circ$ latitude of the same area. Although control points from DOD-66 and the ACIC/AMS nets are input to the computational program, they are generally not used in the adjustment. They are merely compared to the control established by Lunar Orbiter IV and the root mean square differences are output in the statistical summary. Preliminary results have shown a bias between the two systems of approximately two kilometers, but the final results have yet to be published.

All of these control systems are steps toward the fulfillment of the essential requirements for the development of geodetic and cartographic knowledge of the moon as outlined by the Falmouth conference of scientists, convened by the National Aeronautics and Space Administration at Falmouth, Massachusetts in July of 1965 [12]. Among these requirements are:

Establish a selenodetic coordinate system... related
to the right ascension/declination system.

Derive a reference figure with respect to a point which is representative of the moon's center of mass.

Establish a three-dimensional geodetic control system... in terms of latitude, longitude, and height above the chosen reference figure.

These requisites are not only essential to the expansion of geodetic and cartographic knowledge of the moon, but become fundamental, base knowledge for the exercise of other disciplines [12]. Photogrammetry has demonstrated uniquely that it provides the necessary capability to efficiently gather the necessary data and to process it into useful and meaningful information [12].

The following photogrammetric procedure is submitted as a modest contribution to the ever expanding numbers of methods designed to increase man's knowledge of the lunar body.

4. EXPERIMENTATION

4.1 Real Data Experiment

4.1.1 Preliminary

The purpose of this demonstration is to describe in detail the procedure utilized to transfer local or selenographic coordinates from an assumed or known location to surrounding lunar features that are identifiable in orbital photographs. It must be realised, however, that no lunar surface photography has been accomplished with this purpose in mind. As a result several basic assumptions are employed and various procedures inaugurated that would normally be unnecessary were such a mission assigned to personnel of the APOLLO series or follow-on series which would reach the lunar surface.

4.1.2 Materials

The following materials, equipment, and systems were used:

- A. APOLLO 12 Lunar Surface Photographs; AS12-48-7090, 7091, 7092; Magazine X; Exposed by a 70mm Hasselblad camera with focal plane reseau grid. (Nominal focal length, 60mm)
- B. A.M.S., Lunar Map, Surveyor III Site; Scale; 1:2000 (1st ed., Jan 1968)
- C. Mann Precision Comparator, Type 735 with Mann Data Logger
- D. IBM 360/75 Computer System (OSU installation)

The photographs identified in A. above were the result of an extensive search of all surface photography obtained during the surface operations of Apollo Missions XI and XII. They were selected with the following criteria in mind:

- A. Stereoscopic coverage
- B. Maximum base between photographs
- C. Simultaneous; photographic coverage of the LM, Surveyor III; and other points on the lunar surface that could be identified from orbital photography

D. Exposed with a calibrated camera equipped with a focal plane, reseau grid.

These three photos fulfilled these requirements adequately with an average base estimated to be twenty meters; the LM and Surveyor III were imaged on each photo; three relatively well defined lunar features were imaged; and a post flight calibration was conducted on the two cameras employed. Each camera was equipped with reseau grid at the focal plane. Unfortunately, it has not been ascertained which camera exposed these particular plates [4]. However, their calibrated focal lengths of 61.547mm (#1016) and 61.636mm (#1002) determined at a 22.5m focus with black and white film (KODAK S0267) were quite similar [5][6]. Neither camera had a lens distortion pattern that would require consideration except for the most rigorous photogrammetric procedures [5][6].

For the purpose of this demonstration the average focal length was used in calculations. This constituted the introduction of approximately $\pm 0.07\%$ error in the focal length and a proportional amount in the computations associated with it. This was considered insignificant for the purpose of the real data experimentation. Further the reseau grid was assumed to be at exactly spaced internals of 10mm, (4), and radial and tangential distortions were neglected [17][5][6].

4.1.3 Procedure

Broad exposure to the many hundreds of photographs taken during APOLLO XII surface operations permitted the viewer to acquire a semblance of orientation in regard to several features on the lunar surface. This was not facilitated by any documentation concerning time, direction of exposure, orientation of the camera or any other details except in the most general sense. Nevertheless, this orientation permitted the selection of three photographs with the LM, the Surveyor III and three other photoidentifiable features which could be located on the lunar maps. Further, it was confirmed that these features could be seen on available orbital photography. Specifically, this was photography from Lunar Orbiters I and III. APOLLO XII orbital photography which

covered Surveyor III Site was taken at a height of approximately 60 nautical miles using a lens of 80mm focal length. The comcomittant photo scale was nearly 1:1,400,000. This was entirely inadequate for surface feature identification within the limitations of surface acquired photography.

The lunar maps of Site III were employed to establish the coordinates of the five points to be used. The LM was plotted on Lunar Map, Surveyor III Site (Scale; 1:2000) from coordinates established on Lunar Surface Exploration Map, LSE 7-6, Scale 1:5000, prepared by the U.S. Army Topographic Command, 1 November 1969. With the top, center of the LM arbitrarily defining the origin of a local cartesian coordinate system its azimuth from Surveyor III was measured on map B as 301° 30' 00".0 and fixed to establish orientation. Additionally, the distance between the LM and Surveyor was measured and fixed at 202.00 meters to establish scale. The local coordinates of the three other points were obtained relative to the LM. The heights were determined relative to the top center of the LM by interpolating between the five meter supplementary contour intervals provided on the map. The initial locations of all points are summarized as follows (See Figures I, IA, and II):

<u>POINT</u>	<u>SELENOGRAPHIC COORDS.</u>		<u>LOCAL CARTESIAN COORDS.</u>		
	<u>LATITUDE</u>	<u>LONGITUDE</u>	<u>X</u>	<u>Y</u>	<u>Z</u>
1 (LM)	3-11-51.6 S	23-23-14.6 W	1000.00	1000.00	100.00
2 (SURVEYOR)	3-12-04.0 S	23-22-53.6 W	1172.23	894.46	87.49
3 (MOUND)	3-11-46.1 S	23-23-20.3 W	948.00	1045.00	93.96
4 (LONE ROCK)	3-11-52.9 S	23-22-58.8 W	1129.23	988.46	93.96
5 (CRATER RK)	3-11-53.5 S	23-22-55.7 W	1156.23	982.46	91.96

The location of camera exposure stations provided a more difficult problem since there was no documentation in their regard. Therefore, estimated positions had to be determined from the photographs themselves. This was accomplished graphically by constructing a template based on the camera field of view. With a nominal focal length of 60 millimeters and usable camera format of 52 by 52 millimeters the angular field of view was computed to be

approximately 46°. There was an angular field of 9.2° between adjacent reseau crosses. The template was overlayed on the lunar map and adjusted until identifiable lunar features were in their proper angular relationship. When the optimum fitting of the template was achieved, the vertex defined approximations of the exposure station in planimetry (X_o, Y_o) and the central axis of the template defined the direction of the camera optical axis. This provided an estimate for the phi (ϕ) rotation. Exposure station height (Z_o) was again interpolated from contour intervals modified by an added 1.37 meters based on the assumption that the astronaut accomplished the photography standing with the camera at mid-chest level. Estimates of the omega (ω) and kappa (κ) rotations were determined from the apparent depression angle of the center cross reseau and the comparison of a line of horizontal reseau marks with the apparent lunar horizon, respectively. A summary of the locations of the exposure stations and camera orientation estimates are (See Figures I, IA, and II):

<u>STATION</u>	<u>SELENOGRAPHIC COORDS.</u>		<u>LOCAL CARTESIAN COORDS.</u>		
<u>(PHOTO#)</u>	<u>LATITUDE</u>	<u>LONGITUDE</u>	<u>X_o</u>	<u>Y_o</u>	<u>Z_o</u>
1 (7090)	3° 12 ' 11.3 S	23° 22 ' 52.0 W	1186.23m	832.46m	94.09m
2 (7091)	3 12 09.0 S	23 22 49.6 W	1206.23	852.96	94.24
3 (7092)	3 12 06.7 S	23 22 48.6 W	1214.73	871.46	95.34

<u>ORIENTATION (DEGREES/RADIANS)</u>			
	<u>κ</u>	<u>ϕ</u>	<u>ω</u>
1	3.50 / 0.06109*	20.0 / 0.34907	80.0 / 1.39626*
2	3.50 / 0.06109	42.0 / 0.73304	80.0 / 1.39626
3	3.50 / 0.06109	60.0 / 1.04720	80.0 / 1.39626

* A selected average for the three photographs was employed for the κ and ω rotations.

It became apparent during the template fitting procedure that there existed a definite possibility of a significant discrepancy between the location

SURVEYOR III SITE

SCALE 1:2000

MERCATOR PROJECTION

STANDARD PARALLELS AT 2°30'N AND 2°30'S LATITUDES

CONTOUR INTERVAL—10 METERS

SUPPLEMENTARY CONTOURS AT 5 METER INTERVALS

CONTOURS AND SPOT ELEVATIONS ARE EXPRESSED AS RADIUS VECTORS IN METERS WITH THE FIRST THREE DIGITS OMITTED. FOR EXAMPLE: A RADIUS VECTOR OF 1738250 METERS IS DESIGNATED 8250 METERS.

THE VERTICAL AND HORIZONTAL CONTROL NETWORK ON THIS MAP WAS ESTABLISHED BY PHOTOGRAMMETRIC TRIANGULATION USING THE LUNAR ORBITER SITE IP-7 CONTROL.

RELATIVE ERRORS EXPRESSED IN METERS (90 PERCENT PROBABILITY)

HORIZONTAL	3 METERS
VERTICAL	6 METERS



Figure I

Figure 1A

Figure II. (Photo AS12-48-7092)

plotted for the LM and the position indicated by its angular relationship with other features. It appeared that the actual position of the LM should be some 25 meters to the NE of its current position. However, since no better information on its selenographic coordinates was available. It was considered to be fixed with the qualification that this discrepancy would be investigated by varying the application of constraints on it and other points during the adjustment.

The original intention was to measure photo coordinates on the Zeiss, Precision Stereocomparator, PSK, with ancillary IBM 026 card punch to facilitate use of the computer program COMCORDCON. This program converts comparator coordinates to photo coordinates by an affine transformation, simultaneously correcting for lens distortion and film shrinkage (See Appendix I). Because of the malfunction of this equipment the Mann Precision Comparator was utilized. Unfortunately, to simplify the observation procedure, each plate was rotated approximately 30° to prevent alignment of the measuring cross with the photographic reseau crosses. This prohibited COMCORDCON from properly identifying the four reseau marks associated with each point measured and correlating them to the reseau, photo-coordinate system. A simple, two-point transformation routine was employed to rotate the comparator coordinate system near enough to the reseau photo-coordinate system to make the data compatible to COMCORDCON. The output from COMCORDCON was then ready for input to the BLOCK TRIANGULATION computer program (See Appendix II).

The following mean standard errors were estimated for conversion to the variance-covariance matrices for subsequent use in the BLOCK TRIANGULATION program for weighting:

Photo coordinates;	$\hat{\sigma}_x = \hat{\sigma}_y = 0.01 \text{ mm}$
Exterior orientation;	$\hat{\sigma}_{x_o} = \hat{\sigma}_{y_o} = \hat{\sigma}_{z_o} = 20.0 \text{ m}$
	$\hat{\sigma}_\omega = \hat{\sigma}_\psi = 0.174533 \text{ rad } (10^\circ)$
	$\hat{\sigma}_\kappa = 0.08727 \text{ rad } (5^\circ)$
Survey coordinates;	$\hat{\sigma}_x = \hat{\sigma}_y = \hat{\sigma}_z = \infty \text{ to } 0.01 \text{ m (various)}$

4.1.4 Real Data Results

In addition to the variance-covariance matrices postulated from the standard errors of the previous section, constraints on the survey coordinates of Points 1 and 2 and the elevation coordinate of Point 3 were imposed assuming a standard error of 0.01 meter. The results of this first adjustment were exceedingly poor. Subsequent adjustments consisted of input imposing constraints on combinations of Points 1 and 2 and variable constraints and relaxations on Points 3, 4, and 5. These triangulations either provided only slightly improved results or the adjustment failed to converge at all.

Two tendencies were manifest, particularly. Point 1, the LM, continually drifted to the lunar northeast or east, and there was a constant warping of the model most evident in the residuals on surface point elevations, the κ rotation which was constrained to 5° , and in ω which was constrained to 10° . When the constraints on Point 1 were relaxed, the LM freely moved approximately 48 meters almost due east of its initially plotted position. The warping appeared to subside to some extent, but further variations of the weight matrices were required to reduce the residuals on survey elevations and the rotations associated with the elements of exterior orientation to any degree of realism or consistency.

These difficulties were attributed to the possibly erroneous positioning of Point 1, the possible misidentification of Point 3, and the uncertainties associated with the coordinates of all points that were fixed and employed as control for the model. Elevation differences were particularly noted to be a potential source of error since the elevation differences among all points were relatively small and generally within the predicted error of the lunar map (6 meters with 90% probability). A further complicating factor involved with the uncertainties in elevation determination and the minimal differences was the near coplanearity of the control. As explained by Smith [29] this would manifest itself in the triangulation program as an indeterminacy of the normal coefficient matrix. Of possibly worse consequence is Thompson's [31]

expansion of Smith's explanation which would indicate, if not indeterminacy, then an instability of the solution.

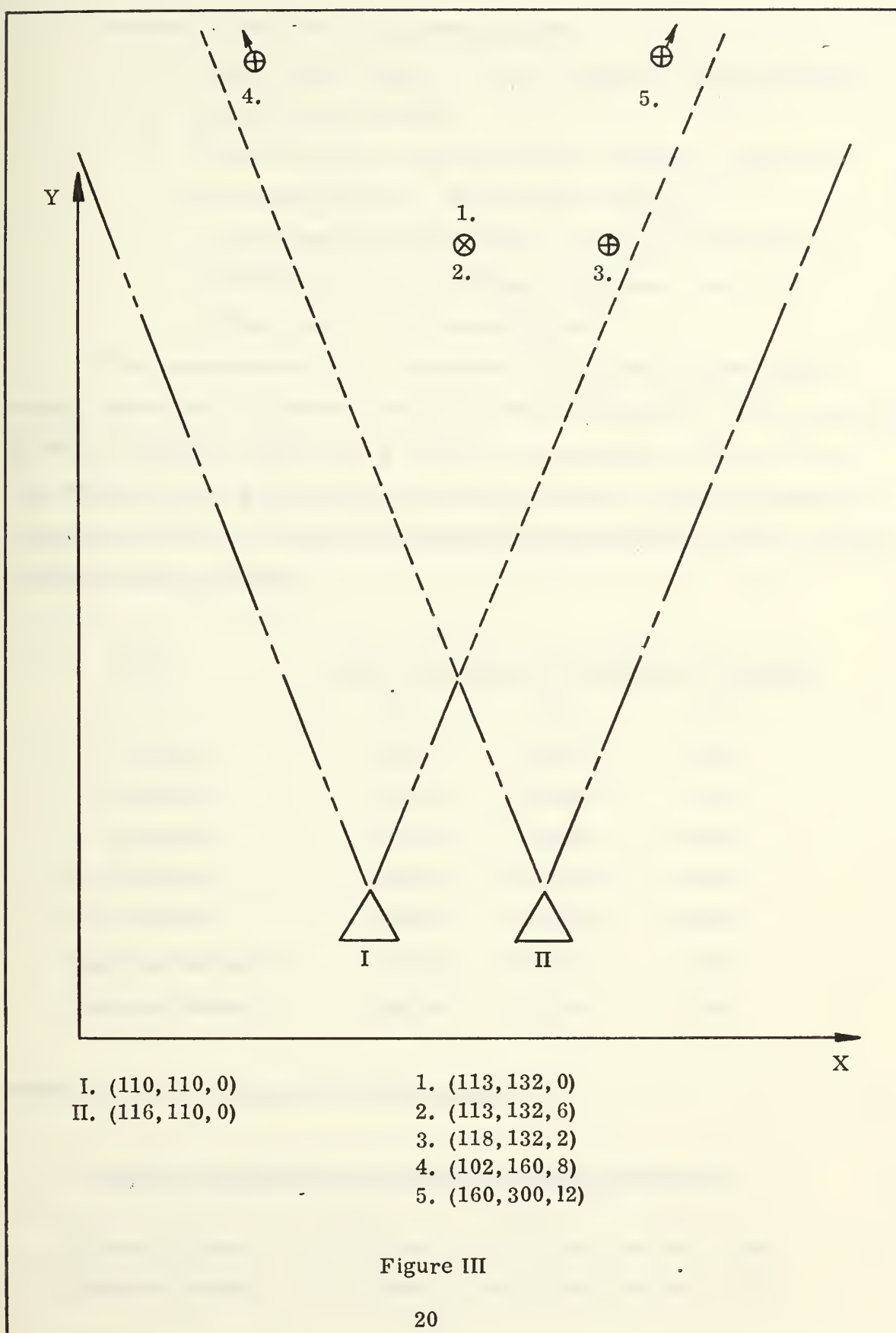
Triangulations numbered 27 and 29 provided the most consistent adjustments that could be extracted from the real data. However, No. 27 utilized Point 3 as a control point and, as a result, the values involved must be suspect. Triangulation No. 29 utilized Points 2, 4, and 5. Since these points appeared to be well identified, were in proximity to the camera exposure stations, and had the best known positional relationship, this triangulation is accepted as the most valid. Unfortunately, acceptance of triangulation No. 29 positions the LM at LAT. 3-11-51.4 S LONG. 23-23-08.1 W. This reduces the distance between the LM and Surveyor III to approximately 163 meters, and redefines the bearing to the LM to about $311^{\circ} 30'$. This possible redefinition of the scale and orientation of the system effectively distorts the information it produces. Nevertheless, the results do have value insofar as the adjustment retains consistency and merely lacks a valid scale and orientation. A complete summary of the results and the statistics of these adjustments are provided on pages 25 through 36.

It can be concluded that the possible gross uncertainties of this particular set of real data negate any reasonable expectation of significant results. However, the feasibility of employing real data with proper control seems to be reasonably apparent.

4.2 Idealized Data Experiment

4.2.1 Procedure

In order to provide a standard by which one might logically anticipate the predicted accuracies of a triangulation program utilizing lunar surface photography with realistic control, an idealized model was constructed (Figure III). This model presupposes a reasonable capability of determining the relative elevations of Point 3 and the camera exposure stations with respect to Points 1 and 2; and an ability to make an estimate of the κ and ω rotations of the elements of exterior orientation.



Additional conditions and parameters are:

1. Points 1 and 2 aligned with local vertical at a fixed distance
(In this case 6 meters)
2. Point 3 at a known elevation relative to Points 1 and 2 and
at a known distance. (In this case 5 meters)
3. A Hasselblad camera (described previously) utilized for at
least two exposures providing a stereoscopic pair at a
distance near its 22.4 meter focus.

The coordinates of Point 1 (assumed to be an LM or other similar landing vehicle) are considered fixed and to define the origin of a local cartesian coordinate system. Points 1 and 2 define the Z survey axis; and Point 3 is then defined to be on a line parallel to the X survey axis. The coordinates of the control points (1, 2, and 3), the photoidentifiable features (4 and 5), and the exposure stations become:

<u>POINT</u>	<u>LOCAL CARTESIAN COORDINATES (meters)</u>		
	<u>X</u>	<u>Y</u>	<u>Z</u>
1. (Target)	113.00	132.00	0.00
2. (Target)	113.00	132.00	6.00
3. (Target)	118.00	132.00	2.00
4. (Feature)	102.00	160.00	8.00
5. (Feature)	160.00	300.00	12.00
Exposure Station 1	110.00	110.00	0.00
Exposure Station 2	116.00	110.00	0.00

And the rotational orientations of the cameras is:

<u>CAMERA ORIENTATION ANGLES (DEGREES/RADIANS)</u>			
	κ	ϕ	ω
Exposure Station 1	0.00/0.0000	0.00/0.0000	90.00/1.5708
Exposure Station 2	0.00/0.0000	0.00/0.0000	90.00/1.5706

The estimated standard errors associated with the various observations are:

Photo coordinate : $\sigma_x = \sigma_y = 0.005$ millimeters

Survey coordinates

Targets : $\sigma_x = \sigma_y = \sigma_z = 0.01$ meters

Features: $\sigma_x = \sigma_y = \sigma_z = \infty$ meters

Exposure Station : $\sigma_x = \sigma_y = \infty$ meters

$\sigma_z = 0.01$ meters

$\sigma_\chi = 0.08727$ radians (5°)

$\sigma_\phi = \sigma_\omega = 0.17453$ radians (10°)

4.2.2 Idealized Data Results

The initial adjustment of the idealized data was a slight modification from that which is tabulated. The first triangulation constrained the survey coordinates in relation to the relative errors of the lunar map. This was assumed to provide standard errors of $\sigma_{x_0} = \sigma_{y_0} = 3$ meters and $\sigma_{z_0} = 6$ meters.

Although the results of the first adjustment produced smaller standard errors in the adjusted coordinates of the photoidentifiable features, the realism of estimating the X_0 and Y_0 of the camera exposure stations on the lunar surface to that accuracy appeared questionable. On the other hand the estimate of elevation differences between the camera stations and Points 1 and 2 to a reasonable accuracy seemed practicable. As a result, constraints on X_0 and Y_0 were removed and that on Z_0 was strengthened. These results were predictably good and are provided on pages 37 through 42.

In an effort to produce results that might be more indicative of those that could be achieved in actual lunar surface operations, the coordinates of the surface features were perturbed within the limits of the map accuracy. Expectedly, the results were identical. In a subsequent adjustment the constraints on the photo-coordinates were relaxed; that is, the weight on photo-coordinates was reduced from 40,000 to 10,000 ($\sigma_{x,y} = 0.010$ millimeters vice 0.005 millimeters). This caused a significant deviation of the adjusted

coordinates of the lunar features from the known positions. In turn, the constraints on the rotations of the exterior orientation elements were relaxed, and the camera constant was perturbed by an additive 0.050 millimeters. The following table provides these results for comparison.

Condition I: Coordinates of Points 1, 2, and 3 constrained to 0.01 meter; Z_0 to 0.01 meter; κ to 5° ; ϕ and ω to 10° ; photo-coordinates to 5 microns; and $f = 60.0$ millimeters

II: All of the above except photo-coordinates constrained to 10 microns

III: Same as II except constraints on κ , ϕ , and ω removed.

IV: Same as III except f perturbed ($f = 60.050$ millimeters)

CONDITION	ADJUSTED COORDINATES			FEATURE POINT NUMBER
	x	y	z	
KNOWN	102.00	160.00	8.00	4
I	102.009	159.991	7.998	4
II	102.010	159.977	7.996	4
III	102.010	159.977	7.996	4
IV	102.010	160.001	7.996	4
KNOWN	160.00	300.00	12.00	5
I	159.990	299.803	11.986	5
II	159.907	299.514	11.967	5
III	159.908	299.518	11.968	5
IV	159.908	299.657	11.968	5

It can be seen that the most significant deviation of the adjusted coordinates from the known coordinates of the feature occurs as a result of relaxing the constraints on the photo-coordinates. This is not unexpected since there is a large weight change involving the elements which provide the basic control for the model. The only other significant deviation is noted when the focal length of the camera is perturbed and this is apparently confined to the y survey coordinate which coincides with the rotated camera z axis.

The following table shows the results of the experiments conducted on the effect of the concentration of the solution on the rate of reaction. The concentration of the solution was varied from 0.1 M to 0.5 M, and the rate of reaction was measured by the volume of gas evolved per unit time. The results show that the rate of reaction increases with increasing concentration of the solution.

The following table shows the results of the experiments conducted on the effect of the temperature of the solution on the rate of reaction. The temperature of the solution was varied from 20°C to 40°C, and the rate of reaction was measured by the volume of gas evolved per unit time. The results show that the rate of reaction increases with increasing temperature of the solution.

Experiment 1: Effect of Concentration					Concentration (M)
0.1	0.2	0.3	0.4	0.5	0.1
0.1	0.2	0.3	0.4	0.5	0.2
0.1	0.2	0.3	0.4	0.5	0.3
0.1	0.2	0.3	0.4	0.5	0.4
0.1	0.2	0.3	0.4	0.5	0.5
Experiment 2: Effect of Temperature					Temperature (°C)
20	30	35	40	45	20
20	30	35	40	45	30
20	30	35	40	45	35
20	30	35	40	45	40
20	30	35	40	45	45

The following table shows the results of the experiments conducted on the effect of the surface area of the solid reactant on the rate of reaction. The surface area of the solid reactant was varied from 1 cm² to 10 cm², and the rate of reaction was measured by the volume of gas evolved per unit time. The results show that the rate of reaction increases with increasing surface area of the solid reactant.

Although the scope of this investigation inhibits specific predictions of accuracy, it appears that with proper control on Points 1, 2, and 3 and the Z_0 of the exposure stations a calibrated camera is capable of producing positional accuracies of lunar features to several tenths of meters at distances of approximately three-hundred meters from the control. The limited number of points negates any empiric estimate concerning the relationship between positional error and distance from the established control.

THE UNIVERSITY OF CHICAGO
DIVISION OF THE PHYSICAL SCIENCES
DEPARTMENT OF CHEMISTRY
530 SOUTH EAST ASIAN AVENUE
CHICAGO, ILLINOIS 60607
TEL: 773-936-5000 FAX: 773-936-5001
WWW.CHEM.UCHICAGO.EDU

THE UNIVERSITY OF CHICAGO
DIVISION OF THE PHYSICAL SCIENCES
DEPARTMENT OF CHEMISTRY
530 SOUTH EAST ASIAN AVENUE
CHICAGO, ILLINOIS 60607
TEL: 773-936-5000 FAX: 773-936-5001
WWW.CHEM.UCHICAGO.EDU

SURVEYOR III SITE ADJUSTMENT

JOB NUMBER 27

DATE 13 AUG. 1970

TIME 15:57:58.2

NUMBER OF PHOTOS = 3

DEGREES OF FREEDOM = 18

UNIT STANDARD ERROR = 0.68304D 00

RESULTS
EXTERIOR ORIENTATION

PHOTO NO. 1	X0 (METERS)	Y0 (METERS)	Z0 (METERS)	KAPPA (RAO.)	PHI (RAO.)	OMEGA (RAO.)
	1183.716	550.988	92.701	0.1230960 00	0.3669200 00	0.1426610 01
STD. ERROR	0.14950-01	0.68170-01	0.14960-01	0.26760-03	0.13270-03	0.14430-03
RESIDUALS	0.25140 01	-0.18530 02	0.13840 01	-0.62010-01	-0.17850-01	-0.30350-01
WEIGHTS	0.003	0.003	0.003	131.312	32.828	32.828

VARIANCE/COVARIANCE MATRIX

0.223450-03	-0.871510-03	0.162650-03	-0.748810-06	-0.592010-06	-0.117760-05
-0.871510-03	0.464670-02	-0.800070-03	0.162540-05	0.626960-05	0.529220-05
0.162650-03	-0.800070-03	0.223690-03	-0.132900-05	-0.851390-06	-0.189410-05
-0.748810-06	0.162540-05	-0.132900-05	0.716290-07	-0.893690-08	0.152130-07
-0.592010-06	0.626960-05	-0.851390-06	-0.893690-08	0.176080-07	0.384120-08
-0.117760-05	0.529220-05	-0.189410-05	0.152130-07	0.384120-08	0.208280-07

PHOTO NO. 2	X0 (METERS)	Y0 (METERS)	Z0 (METERS)	KAPPA (RAO.)	PHI (RAO.)	OMEGA (RAO.)
	1192.696	867.427	92.515	0.2116130 00	0.6705940 00	0.1395010 01
STD. ERROR	0.20090-01	0.25800-01	0.80860-02	0.21100-03	0.78030-04	0.10540-03
RESIDUALS	0.13530 02	-0.14470 02	0.17200 01	-0.15050 00	0.62450-01	0.12480-02
WEIGHTS	0.003	0.003	0.003	131.312	32.828	32.828

VARIANCE/COVARIANCE MATRIX

0.403800-03	-0.490360-03	0.120460-03	-0.373910-06	0.635710-06	-0.100140-05
-0.490360-03	0.665510-03	-0.134550-03	0.161900-06	-0.356830-06	0.122690-05
0.120460-03	-0.134550-03	0.654100-04	-0.461220-07	0.132530-06	-0.666280-06
-0.373910-06	0.161900-06	-0.461220-07	0.445160-07	-0.658330-08	-0.343140-08

PHOTO NO. 3	X0 (METERS)	Y0 (METERS)	Z0 (METERS)	KAPPA (RAO.)	PHI (RAO.)	OMEGA (RAO.)
	1215.846	864.897	98.034	0.1971640 00	0.9654370 00	0.1342290 01
STD. ERROR	0.27260 00	0.17410 00	0.79050-01	0.14150-02	0.28270-03	0.51970-03
RESIDUALS	-0.11160 01	0.65630 01	-0.26990 01	-0.13610 00	0.81760-01	0.53970-01
WEIGHTS	0.003	0.003	0.003	131.312	32.828	32.828

VARIANCE/COVARIANCE MATRIX

0.742900-01	-0.470240-01	0.213130-01	-0.210220-04	0.297190-04	-0.131630-03
-0.470240-01	0.303020-01	-0.136500-01	-0.154560-04	-0.130540-04	0.848980-04
0.213130-01	-0.136500-01	0.624840-02	0.469040-05	0.660400-05	-0.395250-04
-0.210220-04	-0.154560-04	0.469040-05	0.200200-05	-0.348090-06	-0.105440-06
0.297190-04	-0.130540-04	0.660400-05	-0.348090-06	0.799130-07	-0.314570-07
-0.131630-03	0.848980-04	-0.395250-04	-0.105440-06	-0.314570-07	0.270070-06

RESULTS

PHOTO COORDINATES
(ALL WEIGHTS TAKEN AS 10000.0)

PHOTO NO.	POINT NO.	X (MM)	Y (MM)	VX (MM)	VY (MM)
1	1	-23.713	12.255	-0.6078D-04	-0.9402D-04
1	2	6.952	0.643	-0.1971D-04	0.2792D-05
1	4	-0.087	7.464	0.2142D-04	0.3449D-03
1	5	10.840	7.235	0.4740D-04	-0.2789D-03
2	1	-7.760	11.538	0.4970D-04	0.3156D-03
2	2	1.768	-0.785	-0.1704D-05	0.3801D-05
2	3	-15.893	10.497	-0.2664D-04	-0.1076D-03
2	4	13.206	6.306	-0.3438D-04	-0.3182D-03
2	5	24.894	5.714	0.1951D-04	0.1263D-03
3	1	6.541	8.583	0.4338D-04	-0.2828D-03
3	2	0.122	-4.210	0.2753D-04	0.4466D-05
3	3	-0.010	7.218	-0.2615D-04	0.2880D-03

RESULTS
SURVEY COORDINATES

POINT NO.	1	X	Y	Z
		1019.420	1029.260	100.595
STD. ERROR		0.1940D 00	0.1867D 00	0.1626D-01
RESIDUALS		-0.1942D 02	-0.2926D 02	-0.5947D 00
WEIGHT		0.0	0.0	0.0

VARIANCE/COVARIANCE MATRIX

0.37620D-01	-0.35991D-01	-0.12927D-02
-0.35991D-01	0.34840D-01	0.12526D-02
-0.12927D-02	0.12526D-02	0.26444D-03

POINT NO.	2	X	Y	Z
		1172.230	894.460	87.490
STD. ERROR		0.3868D-02	0.4949D-02	0.2628D-02
RESIDUALS		0.2624D-04	0.7259D-05	-0.2293D-04
WEIGHT		10000.000	10000.000	10000.000

VARIANCE/COVARIANCE MATRIX

0.14961D-04	-0.12227D-04	0.23358D-05
-0.12227D-04	0.24488D-04	-0.33500D-05
0.23358D-05	-0.33500D-05	0.69086D-05

POINT NO.	3	X	Y	Z
		948.000	1045.000	93.960
STD. ERROR		0.6741D-02	0.6647D-02	0.6561D-02
RESIDUALS		0.5739D-05	0.6810D-05	-0.3354D-04
WEIGHT		10000.000	10000.000	10000.000

VARIANCE/COVARIANCE MATRIX

0.45437D-04	-0.17313D-05	0.51878D-07
-0.17313D-05	0.44188D-04	0.53027D-07
0.51878D-07	0.53027D-07	0.43044D-04

POINT NO.	4	X	Y	Z
		1125.341	996.982	90.448
STD. ERROR		0.9941D-01	0.2125D 00	0.1208D-01
RESIDUALS		0.3889D 01	-0.8522D 01	0.3515D 01
WEIGHT		0.0	0.0	0.0

VARIANCE/COVARIANCE MATRIX

0.98828D-02	-0.20952D-01	0.34245D-03
-0.20952D-01	0.45159D-01	-0.74009D-03
0.34245D-03	-0.74009D-03	0.14588D-03

POINT NO.	5	X	Y	Z
		1156.230	982.460	91.963
STD. ERROR		0.55500-02	0.67380-02	0.55130-02
RESIDUALS		-0.35720-04	-0.74610-05	0.56370-04
WEIGHT		10000.000	10000.000	10000.000

VARIANCE/COVARIANCE MATRIX

0.308000-04	-0.433010-05	-0.382330-06
-0.433010-05	0.454010-04	-0.200130-06
-0.382330-06	-0.200130-06	0.303980-04

SURVEYOR III SITE ADJUSTMENT

JOB NUMBER 29

DATE 13 AUG. 1970

TIME 19:37:25.6

NUMBER OF PHOTOS = 3

DEGREES OF FREEDOM = 18

UNIT STANDARD ERROR = 0.68902D 00

RESULTS
EXTERIOR ORIENTATION

PHOTO NO. 1	X0 (METERS)	Y0 (METERS)	Z0 (METERS)	KAPPA (RAD.)	PHI (RAD.)	OMEGA (RAD.)
	1183.800	853.811	91.759	-0.1534180-01	0.3884060 00	0.1457180 01
STD. ERROR	0.13970-01	0.56720-01	0.12730-01	0.26450-03	0.13170-03	0.14490-03
RESIDUALS	0.24300 01	-0.21350 02	0.23260 01	0.76430-01	-0.39340-01	-0.60920-01
WEIGHTS	0.003	0.003	0.003	131.312	32.828	32.828

VARIANCE/COVARIANCE MATRIX

0.195060-03	-0.663610-03	0.123690-03	-0.540200-05	-0.365720-06	-0.116650-05
-0.663610-03	0.321670-02	-0.536460-03	0.124510-07	0.478630-05	0.468030-05
0.123690-03	-0.536460-03	0.162110-03	-0.799180-06	-0.567450-06	-0.165690-05
-0.540200-05	0.124510-07	-0.799180-06	0.699500-07	-0.125890-07	0.101920-07
-0.365720-06	0.478630-05	-0.567450-06	-0.125890-07	0.173520-07	0.346420-08
-0.116650-05	0.468030-05	-0.165690-05	0.101920-07	0.346420-08	0.209840-07

PHOTO NO. 2	X0 (METERS)	Y0 (METERS)	Z0 (METERS)	KAPPA (RAD.)	PHI (RAD.)	OMEGA (RAD.)
	1194.703	866.420	90.639	0.4682800-01	0.7018820 00	0.1473520 01
STD. ERROR	0.20070-01	0.24160-01	0.72030-02	0.21820-03	0.83230-04	0.11490-03
RESIDUALS	0.11530 02	-0.13460 02	0.35960 01	0.14260-01	0.31160-01	-0.77260-01
WEIGHTS	0.003	0.003	0.003	131.312	32.828	32.828

VARIANCE/COVARIANCE MATRIX

0.402660-03	-0.450560-03	0.838320-04	-0.152550-06	0.693390-06	-0.103990-05
-0.450560-03	0.583620-03	-0.100140-03	-0.197760-06	-0.277940-06	0.121640-05
0.838320-04	-0.100140-03	0.518760-04	0.148770-06	0.100640-06	-0.679110-06
-0.152550-06	-0.197760-06	0.148770-06	0.476240-07	-0.669840-08	-0.709520-08

PHOTO NO. 3	X0 (METERS)	Y0 (METERS)	Z0 (METERS)	KAPPA (RAD.)	PHI (RAD.)	OMEGA (RAD.)
	1224.119	862.715	94.512	-0.3817210-02	0.1016510 01	0.1481900 01
STD. ERROR	0.27240 00	0.15530 00	0.57870-01	0.15900-02	0.32520-03	0.70560-03
RESIDUALS	-0.93890 01	0.87450 01	0.82270 00	0.64910-01	0.30690-01	-0.85640-01
WEIGHTS	0.003	0.003	0.003	131.312	32.828	32.828

VARIANCE/COVARIANCE MATRIX

0.741760-01	-0.416020-01	0.152190-01	0.731960-04	0.409460-04	-0.173610-03
-0.416020-01	0.241290-01	-0.879790-02	-0.800340-04	-0.151270-04	0.102770-03
0.152190-01	-0.879790-02	0.334920-02	0.319650-04	0.558910-05	-0.397240-04
0.731960-04	-0.800340-04	0.319650-04	0.252950-05	-0.374760-06	-0.543120-06
0.409460-04	-0.151270-04	0.558910-05	-0.374760-06	0.105730-06	-0.372210-07
-0.173610-03	0.102770-03	-0.397240-04	-0.543120-06	-0.372210-07	0.497900-06

RESULTS
PHOTO COORDINATES
(ALL WEIGHTS TAKEN AS 10000.0)

PHOTO NO.	POINT NO.	X (MM)	Y (MM)	VX (MM)	VY (MM)
1	1	-23.713	12.255	-0.22290-03	-0.36730-02
1	2	6.952	0.643	-0.20850-04	0.54870-04
1	4	-0.087	7.464	-0.70330-03	0.11710-01
1	5	10.840	7.235	0.84370-03	-0.80570-02
2	1	-7.760	11.538	0.35870-03	0.37840-02
2	2	1.768	-0.785	0.15680-04	-0.49840-04
2	3	-15.893	10.497	-0.54090-04	0.12200-03
2	4	13.206	6.306	0.11220-03	-0.11280-01
2	5	24.894	5.714	-0.32180-03	0.73490-02
3	1	6.541	8.583	-0.84710-04	0.10220-03
3	2	0.122	-4.210	0.42740-05	0.66640-05
3	3	-0.010	7.218	0.78160-04	-0.13900-03

RESULTS
SURVEY COORDINATES

POINT NO.	1	X	Y	Z
		1048.824	1001.120	112.970
STD. ERROR		0.1373D 00	0.1305D 00	0.2267D-01
RESIDUALS		-0.4882D 02	-0.1120D 01	-0.1291D 02
WEIGHT		0.0	0.0	0.0

VARIANCE/COVARIANCE MATRIX

0.18839D-01	-0.17755D-01	-0.25725D-02
-0.17755D-01	0.11028D-01	0.24522D-02
-0.25725D-02	0.24522D-02	0.51397D-03

POINT NO.	2	X	Y	Z
		1172.230	894.460	87.490
STD. ERROR		0.3915D-02	0.5040D-02	0.2643D-02
RESIDUALS		0.1376D-05	-0.1541D-04	-0.2447D-05
WEIGHT		10000.000	10000.000	10000.000

VARIANCE/COVARIANCE MATRIX

0.15326D-04	-0.12281D-04	0.15018D-05
-0.12281D-04	0.25407D-04	-0.22320D-05
0.15018D-05	-0.22320D-05	0.69853D-05

POINT NO.	3	X	Y	Z
		1017.025	993.015	111.559
STD. ERROR		0.4686D 00	0.3176D 00	0.5079D-01
RESIDUALS		-0.6903D 02	0.5198D 02	-0.1760D 02
WEIGHT		0.0	0.0	0.0

VARIANCE/COVARIANCE MATRIX

0.21961D 00	-0.14850D 00	-0.22313D-01
-0.14850D 00	0.10086D 00	0.15119D-01
-0.22313D-01	0.15119D-01	0.25198D-02

POINT NO.	4	X	Y	Z
		1129.230	988.460	93.963
STD. ERROR		0.6033D-02	0.6703D-02	0.5832D-02
RESIDUALS		0.8837D-04	-0.8057D-05	0.1312D-03
WEIGHT		10000.000	10000.000	10000.000

VARIANCE/COVARIANCE MATRIX

0.36401D-04	-0.52303D-05	-0.21482D-06
-0.52303D-05	0.44931D-04	0.18533D-06
-0.21482D-06	0.18533D-06	0.34015D-04

POINT NO.	5	X	Y	Z
		1156.230	982.460	91.963
STD. ERROR		0.5596D-02	0.6790D-02	0.5568D-02
RESIDUALS		-0.9089D-04	0.2998D-04	-0.1304D-03
WEIGHT		10000.000	10000.000	10000.000

VARIANCE/COVARIANCE MATRIX

0.31319D-04	-0.45488D-05	-0.32284D-06
-0.45488D-05	0.46101D-04	0.18323D-07
-0.32284D-06	0.18323D-07	0.31001D-04

JOB NUMBER	0
<hr/>	
DATE 12 AUG. 1970	
TIME 11:39: 3.3	
<hr/>	
NUMBER OF PHOTOS =	2
DEGREES OF FREEDOM =	10
<hr/>	
UNIT STANDARD ERROR =	0.65281D-02

RESULTS
EXTERIOR ORIENTATION

PHOTO NO.	1	XO (METERS)	YO (METERS)	ZO (METERS)	KAPPA (RAO.)	PHI (RAO.)	OMEGA (RAO.)
		109.995	110.002	0.000	-0.1957830-04	-0.2416350-03	0.1570600 01
STO. ERROR		0.17440-04	0.38710-04	0.15110-04	0.12320-05	0.51410-06	0.52180-06
RESIDUALS		-0.99460 00	0.99850 00	-0.44100-04	0.19580-04	0.24160-03	0.34670-05
WEIGHTS		0.0	0.0	10000.000	131.312	32.828	32.828

VARIANCE/COVARIANCE MATRIX

0.304080-09	0.370520-09	0.367630-10	0.238570-11	0.707660-11	0.697200-13
0.370520-09	0.149820-08	0.140370-09	0.183740-11	0.314390-11	0.146610-11
0.367630-10	0.140370-09	0.228340-09	-0.348510-11	0.702740-12	-0.615890-11
0.238570-11	0.183740-11	-0.348510-11	0.151880-11	-0.101370-12	-0.100170-12
0.707660-11	0.314390-11	0.702740-12	-0.101370-12	0.264290-12	0.810650-14
0.697200-13	0.146610-11	-0.615890-11	-0.100170-12	0.810650-14	0.272270-12

PHOTO NO.	2	XO (METERS)	YO (METERS)	ZO (METERS)	KAPPA (RAO.)	PHI (RAO.)	OMEGA (RAO.)
		115.996	110.000	-0.000	-0.1547180-04	-0.1964960-03	0.1570800 01
STO. ERROR		0.14150-04	0.41720-04	0.15520-04	0.12370-05	0.50090-06	0.52240-06
RESIDUALS		-0.29960 01	-0.23440-03	0.39360-04	0.15470-04	0.19650-03	0.41630-05
WEIGHTS		0.0	0.0	10000.000	131.312	32.828	32.828

VARIANCE/COVARIANCE MATRIX

0.200110-09	-0.745440-10	-0.176870-11	0.189810-11	0.577880-11	-0.225200-12
-0.745440-10	0.174030-08	0.161900-09	-0.934620-12	0.215060-11	0.193790-11
-0.176870-11	0.161900-09	0.240780-09	0.537830-11	-0.166670-12	-0.672370-11
0.189810-11	-0.934620-12	0.537830-11	0.152970-11	-0.110780-12	-0.103640-12

RESULTS
PHOTO COORDINATES
(ALL WEIGHTS TAKEN AS 40000.0)

PHOTO NO.	POINT NO.	X (MM)	Y (MM)	VX (MM)	VY (MM)
1	1	8.182	0.0	-0.9879D-05	-0.9001D-05
1	2	8.182	16.364	0.1526D-04	0.5686D-05
1	3	21.818	5.455	-0.5378D-05	0.1655D-05
1	4	-9.600	9.600	0.6378D-11	-0.7707D-05
1	5	15.789	3.789	-0.3272D-10	0.8703D-05
2	1	-8.182	0.0	0.1672D-05	0.8378D-05
2	2	-8.182	16.364	-0.1396D-04	-0.1442D-04
2	3	5.455	5.455	0.1229D-04	0.7265D-05
2	4	-16.800	9.600	-0.3039D-10	0.7707D-05
2	5	13.895	3.789	0.2178D-10	-0.8703D-05

RESULTS
SURVEY COORDINATES

POINT NO.	1	X	Y	Z
		113.000	132.000	-0.000
STD. ERROR		0.8392D-05	0.4497D-04	0.8392D-05
RESIDUALS		0.8954D-04	-0.1721D-04	0.6794D-05
WEIGHT		10000.000	10000.000	10000.000

VARIANCE/COVARIANCE MATRIX

0.70430D-10	0.42722D-12	0.31048D-17
0.42722D-12	0.20226D-08	-0.82362D-15
0.31048D-17	-0.82362D-15	0.70429D-10

POINT NO.	2	X	Y	Z
		113.000	132.000	6.000
STD. ERROR		0.8392D-05	0.4421D-04	0.1453D-04
RESIDUALS		-0.1415D-04	0.1749D-04	0.9527D-04
WEIGHT		10000.000	10000.000	10000.000

VARIANCE/COVARIANCE MATRIX

0.70429D-10	0.42137D-12	0.11716D-12
0.42137D-12	0.19547D-08	0.52430D-09
0.11716D-12	0.52430D-09	0.21106D-09

POINT NO.	3	X	Y	Z
		118.000	132.000	2.000
STD. ERROR		0.1300D-04	0.4436D-04	0.9283D-05
RESIDUALS		-0.7539D-04	-0.2877D-06	-0.9731D-04
WEIGHT		10000.000	10000.000	10000.000

VARIANCE/COVARIANCE MATRIX

0.16894D-09	0.44022D-09	0.39364D-10
0.44022D-09	0.19676D-08	0.17593D-09
0.39364D-10	0.17593D-09	0.86166D-10

POINT NO.	4	X	Y	Z
		102.009	159.991	7.998
STD. ERROR		0.7298D-04	0.3204D-03	0.5475D-04
RESIDUALS		0.1991D 01	-0.1991D 01	0.1502D 01
WEIGHT		0.0	0.0	0.0

VARIANCE/COVARIANCE MATRIX

0.53267D-08	-0.22556D-07	-0.36088D-08
-0.22556D-07	0.10263D-06	0.16421D-07
-0.36088D-08	0.16421D-07	0.29971D-08

POINT NO.	5	X	Y	Z
		159.990	299.803	11.986
STD. ERROR		0.1146D-02	0.4619D-02	0.3007D-03
RESIDUALS		0.3010D 01	0.2197D 01	-0.9858D 00
WEIGHT		0.0	0.0	0.0

VARIANCE/COVARIANCE MATRIX

0.13132D-05	0.52821D-05	0.33356D-06
0.52821D-05	0.21333D-04	0.13472D-05
0.33356D-06	0.13472D-05	0.90404D-07

5. CONCLUSIONS

It is apparent from the results of the real data experiment that, in general, the potential to improve selenodetic control by the use of lunar surface photography exists to a significant degree. Although the specific results are considered inconclusive because of the lack of any dependable, local control, the experiment has emphasized some of the difficulties associated with surface data. Of particular note, is the instability of the solution due to the relative coplanarity of the control utilized. This is a realistic problem when one considers that the APOLLO landing sites to date have been selected in the mare areas where relatively level lunar terrain has been a criteria. It is anticipated that this criteria will continue to be considered, but perhaps, to a lesser extent as the experience in lunar landings is increased. This does, nevertheless, stress the need for good vertical control, strongly constrained, to minimize this instability. Additionally, the solution has manifested a certain sensitivity to the rotations of the camera's elements of exterior orientation. This was particularly evident when all elements of the exposure station were constrained and Points 2, 4, and 5 exercised total control of the model. The resulting adjusted coordinates were realistic only for those points and stations within approximately fifty meters of the control points. The exposure station for photo AS12-48-7090, the most distant of the exposure stations, was almost two hundred meters from its estimated position with more than twenty times the estimated α rotation. Point 3 could not even be plotted on the chart.

On the other hand, the idealized data and that with perturbations provides some indication of the kind of accuracy that may be achieved by a reasonable effort to establish a local network to control the adjustment of more distant features. Further, one may reasonably imply that an additional input of data from overhead photography (properly scaled, if a camera lens of different focal length is employed) would provide a material

improvement to this adjustment. Yet, no specific predictions can be offered because of the paucity of points and the lack of suitable overhead photography and information regarding the lunar conditions (such as surface refraction, etc.). However, it is justifiable to assume that the photogrammetric errors associated with the adjusted local coordinates of lunar features from surface and overhead photography would not contribute materially to the total error substantially attached to any astronomic observations.

6. RECOMMENDATIONS

6.1 Concept

The procedure to be described is a direct application of fundamental geodetic and photogrammetric techniques as described in most textbooks on the subjects. The unique aspect is that these techniques are applied to lunar surface photography supplemented by orbital photography. The basic advantage of this proposal is to establish control where selenodetic control ought to be established...on the lunar surface.

Although this control will be limited in coverage, each subsequent landing will provide a further expansion of the control net with an ever increasing number of points which can be identified from orbit and to which a set of astronomic coordinates originating with the LM may be associated. It is theorized that eventually a net of sufficient extent would be available to effectively control unmanned, orbital photo missions. The following procedure is offered to that end.

6.2 Presupposition

The current lunar landing vehicles are capable of obtaining the astronomic position of the landing site from stellar observations. It is presupposed that this capability will continue and perhaps improve in the accuracy of determination as the APOLLO series progresses. It is further assumed that an azimuth can be determined to relate any local coordinate system to the selenographic system. One method that suggests itself is to image a stellar field on the lunar surface photography related to Universal Time through spacecraft time. This might be accomplished by the use of a half-circular, neutral density filter for the Hasselblad camera. The top, or clear half, would permit sufficient exposure to image the star field while the bottom, or tinted half, would inhibit overexposure of the lunar surface. Time of exposure could be recorded on a magnetic taped voice circuit.

6.3 Equipment

The following equipment is additional to what is carried on the lunar module, and serves only as an example to accomplish the desired procedure.

1. A calibrated tape of approximately 6 meters that can be hung without interference from an available or added projection on the LM. This tape would be targeted at each end with an additional target whose position can be varied and its reading noted. A second, similar target for exposure station reference is optional. It is visualized that they would slide on the tape with friction clamps to maintain their position once established. The lower end should be weighted and might have some dampening device to reduce oscillations.
2. Two lightweight, variable height, telescoping tripods.
 - a. One targeted tripod would be equipped with a small leveling telescope and two calibrated, horizontal spirit levels. One glass parallel to the telescope optical axis, the other normal to it. A plumb bob or optical plumb is necessary.
 - b. The second tripod would provide an attachment for the Hasselblad camera with similarly oriented spirit levels.
3. A calibrated tape of convenient length (perhaps up to 20 meters) with staking rings at each end and a tension spring with scale at one end.

6.4 Procedure

At any specified time during lunar surface excursions, the astronauts would carry out the following procedure:

1. The vertical tape would be hung from the LM.
2. Within 20 meters of the LM on reasonably level terrain that would include a background with a maximum number of discrete features, set up the level telescope in such a manner that it is level and its field encompasses a portion of the vertical tape. Position one of the adjustable targets so that it is centered on the telescope cross hairs.
3. Lay out the 20 meter tape from the base of the vertical tape to a position below the plumb of the level telescope. The tape may be staked in position with a predetermined amount of tension indicated.
4. Position the camera at its first station such that its optical axis is perpendicular to the vertical tape, though not necessarily in the same plane. Include in its field of view, the vertical tape, the targeted level telescope and the desired, discrete lunar features.
5. When the oscillations of the vertical tape are minimal, expose the plate and record:
 - a. The reading on the 20 meter tape below the vertical tape.
 - b. All spirit level bubble positions.
 - c. The reading on the 20 meter tape below the level telescope plumb.
 - d. The readings of the variable target(s) on the vertical tape. (All readings could be voice recorded on tape.)

For subsequent exposures, it would **only** be necessary to reposition the camera to obtain a stereoscopic pair, possibly readjust the optional variable target (if used) and to record the readings already mentioned, (See Figure III).

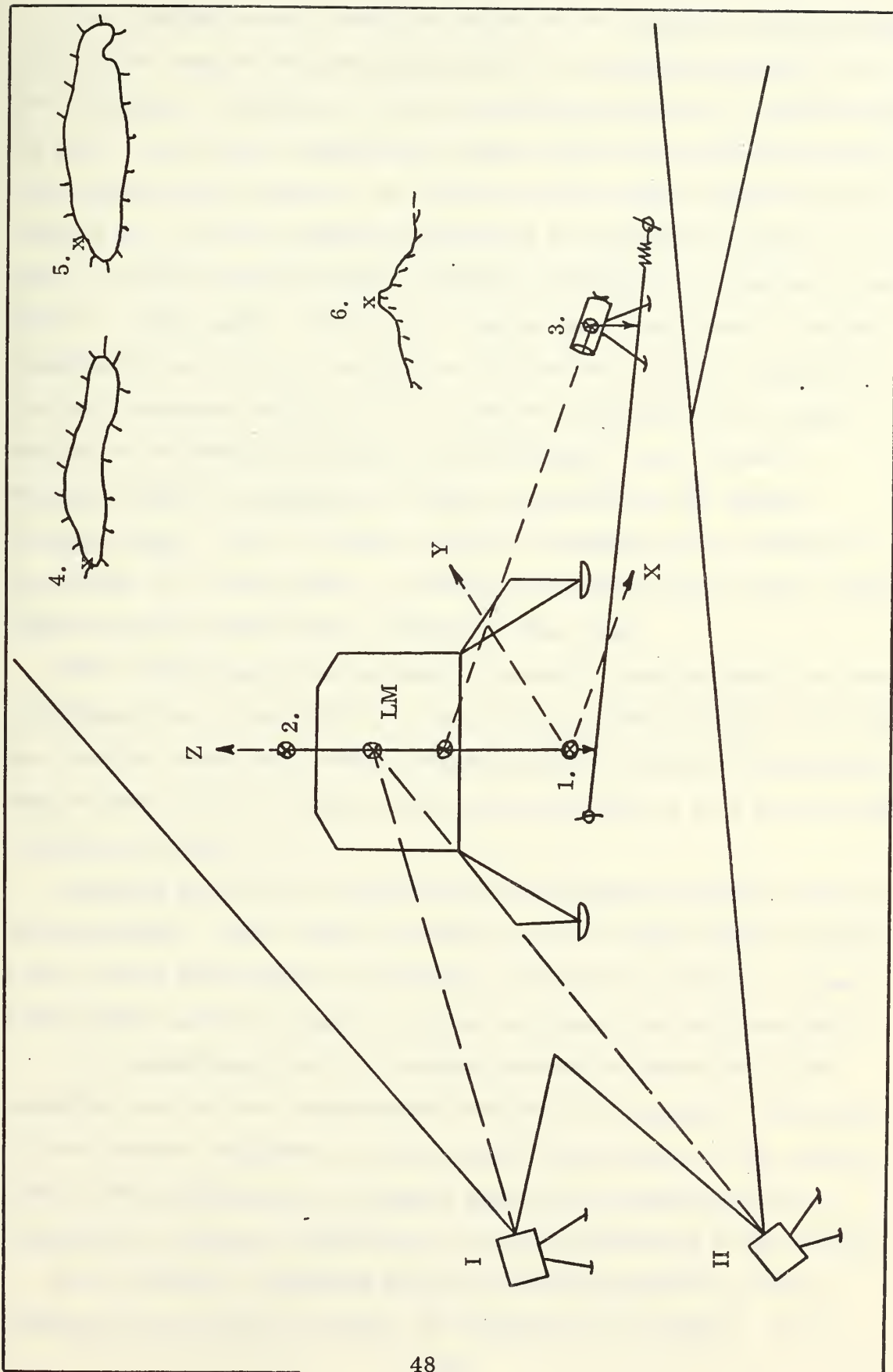


FIGURE III.

The resulting models would be similar to the idealized model described. The vertical tape would provide the scale to an estimated accuracy of a few millimeters and define the local vertical as the local Z survey axis; its lower target would establish the origin of the local coordinate system. The targeted level telescope, the position of the variable target on the vertical tape, and the measured distance to an estimated accuracy of .01 meter, could be computationally corrected to define a line parallel to the local X survey axis. The local Y survey axis would then be defined. Reduction of the recorded readings would give the survey coordinates of the level telescope target and the Z survey coordinate of the camera stations to an estimated accuracy of 0.01 meters. The κ and ω rotations would be estimated to be near zero based on the camera leveling results. The ϕ rotation would be estimated by its relation to the defined YZ survey plane. Approximate positions of the lunar surface features can be scaled from a convenient lunar map.

After preprocessing the necessary information and providing the photo coordinates from COMCORDON to the BLOCK TRIANGULATION PROGRAM, the resulting adjustment would photogrammetrically relate all discretely imaged lunar surface features to the position of the LM in a local cartesian coordinates system.

Extending this with an azimuth and the astronomic position of the LM, this adjustment, with a simple coordinate system transformation program, would provide selenographic coordinates and relative elevations of lunar features that could be related to current and future orbital photography.

It is acknowledged that the foregoing method is neither the most simplified nor the most sophisticated that could be employed. However, it does serve to emphasize the fundamental requirements of the system; that is, the establishment of adequate scale and orientation and the application of sufficient constraints to obviate coplanearity of the model.

It is, therefore, suggested that the previous procedure, or one fulfilling the same basic criteria, be considered for adoption. It is

firmly believed that its implementation would be the beginning of an improved selenodetic control network.

BIBLIOGRAPHY

1. Anonymous. Apollo Mission 12 Lunar Photography Indexes.
Compiled by Mapping Sciences Laboratory, MSC, Houston:
March, 1970.
2. Anonymous. Control Integration for Lunar Mapping. Interim
Report, AMS, NASA Defense Purchase Request No. T-37794 (G).
Washington, D.C.: June, 1966.
3. Anonymous. Evaluation of Lunar Orbiter IV Materials for the
Establishment of a Lunar Geodetic System. ACIC Progress
Report; Defense Purchase Request W-12,500, St. Louis:
ACIC, July, 1968.
4. Baron, G. and Duggan, I. Apollo 12 Photography Index (70mm &
16mm) Technical Working Paper, Project Apollo NASA Contract
NAS 9-5191 LEC/HASD No. TWP-69-044, Houston: December, 1969.
5. Batson, Raymond M. Photogrammetric Calibration Results Lunar
Surface Hasselblad S/N 1016, U.S. Geological Survey, Center of
Astrogeology, Flagstaff, Arizona: July, 1970.
6. Batson, Raymond M. Photogrammetric Calibration Results Lunar
Surface Hasselblad S/N 1002. U.S. Geological Survey, Center
of Astrogeology, Flagstaff, Arizona: July, 1970.
7. Bowles, L.D. & Hardy, Marian. Selenodetic Control for NASA
Project Apollo. Preliminary Report. AMS, NASA Defense
Purchase Request No. T-21657 (G). Washington, D.C.:
March, 1966.
8. Breece, Sam. Horizontal and Vertical Control for Lunar Mapping
(Part Two AMS Selenodetic Control System 1964). Army Map
Service Technical Report No. 29, Washington, D.C.: AMS,
March, 1964.

9. Brown, Duane C. Advanced Methods for the Calibration of Metric Cameras. Paper Prepared for presentation at the 1969 Symposium on Computational Photogrammetry at Syracuse University, January, 1969.
10. Brown D. C. Decentering Distortion and the Definitive Calibration of Metric Cameras. Paper presented at the ASP Convention, March, 1965
11. Conrady, A. E. "Decentered Lens Systems", Monthly Notice of the Royal Astronomical Society, Vol. 79, pp. 384-390, 1919.
12. Doyle, Frederick J. Photogrammetric Geodesy on the Moon. Paper presented at the annual meeting of the American Society of Photogrammetry, March, 1968.
13. Faddeeva, V.N. Computational Methods of Linear Algebra. trans. Curtis D. Benster, New York: Dover Publication, 1959.
14. Ghosh, Sanjib K. Theory of Stereophotogrammetry. Columbus, Ohio, Privately Published, 1968.
15. Goudas, C. L. The Selenodetic Control System of the Aeronautical Chart and Information Center of the U.S. Air Force. Mathematical Note No. 413, Boeing Scientific Research Laboratories: June, 1965.
16. Haines, E.L. Selenodesy and Lunar Dynamics, JPL 900, Jet Propulsion Laboratory, Pasadena: April, 1967.
17. Hallert, B. "A Summary of Preliminary Investigations of the Geometrical Quality of the Camera and Photographs", Hasselblad El Data Camera No. 12123, P/N SEB 33100040 S/N 1004, Manuscript, 1970.

18. Hardy, Marian. Selenodetic Control for NASA Project Apollo, (FA 2.1-1) Interim Report, AMS, NASA Defense Purchase Request No. T-21657(G), Washington, D.C.: AMS, June, 1966.
19. Hathaway, James D. Department of Defense Selenodetic Control System 1966. Final Report, AMS, NASA Defense Purchase Request No. T-37794(G), Washington, D.C.: AMS, January, 1967.
20. Hunt, Mahlon S. and Eckhardt, Donald H. Preliminary Lunar Landmark Location Report, Air Force Cambridge Research Laboratories, L. G. Hanscom Field, Bedford, Massachusetts, September, 1964.
21. James, Robert C. and Glen. James and James Mathematical Dictionary, 3rd Edition, Multilingual Version, Princeton: D. Van Nostrand Company, Inc., 1968.
22. Kopal, Zdenek. Relative Heights of Photographic Features on the Moon, Scientific Report No. 1, Department of Astronomy, University of Manchester, England, USAF Contract F 61052-68-C-002, AFCRL-69-0421, University of Manchester: June, 1969.
23. Meyer, Donald L. and Ruffin, Byron W., Coordinates of Lunar Features Group I and II Solutions, ACIC Technical Paper No. 15, St. Louis: ACIC, March, 1965.
24. Moutsoulas, M. "Star Calibrated Lunar Photography", Relative Heights of Photographic Features of the Moon, ed. Zdenek Kopal, Scientific Report No. 1, Department of Astronomy, University of Manchester USAF Contract F 61052-68-C-0002, AFCRL-69-0421, University of Manchester: June, 1969.
25. Mueller, Ivan I., ed., A General Review and Discussion on Geodetic Control of the Moon, Report #127, Prepared for NASA, MSC, Houston, Texas, Contract No. NAS 9-9695, OSURF Project No. 2841, Columbus, Ohio: 1969.

26. Papo, Haim. "Earth-Based Control", A General Review and Discussion on Geodetic Control of the Moon, ed. Ivan I. Mueller, Report #127, Prepared for NASA, MSC, Houston, Texas, Contract No. NAS 9-9695, OSURF Project No. 2841, Columbus, Ohio: 1969.
27. Ruffin, Byron. A Positional Reference System of Lunar Features Determined From Lunar Orbiter Photography, Contract P.R. W-12374-1, St. Louis: ACIC, May, 1969.
28. Schwidefsky, K. An Outline of Photogrammetry, trans. John Fosberry, New York: Pitman Publishing Corporation, 1959.
29. Smith, A.D.N. "The Explicit Solution of the Single Picture Resection Problem with a Least Squares Adjustment to Redundant Control", Photogrammetric Record, Volume V, October, 1965, p. 113.
30. Stewart, Homer T. "Lunar Exploration: The First Decade Raises More Questions Than It Answers", Lunar Exploration: The Impact of Ranger and Surveyor Results, NASA Technical Report 32-1399, Jet Propulsion Laboratory, Pasadena, Reprinted from Astronautics and Aeronautics, Volume 7, No. 1, January, 1969.
31. Thompson, E.M., "Space Resection: Failure Cases", Photogrammetric Record, Volume V, No. 27, 1966, p. 201.
32. Thompson, Morris M., ed., Manual of Photogrammetry, 3rd Edition, Volume 2, Falls Church: American Society of Photogrammetry, 1966.
33. Zeller, M. Textbook of Photogrammetry, trans. E. A. Miskin and R. Powell, London: H. K. Lewis and Company, Ltd., 1952.

APPENDIX I

COMCORDCON

The purpose of COMCORDCON, an acronym for Computer Coordinate Conversion Program, is, as its name implies, to convert stereoscopic comparator observations of object space points on a photographic plate to photographic coordinates in a photo-coordinate system. The resulting measurements, sequentially corrected for film / emulsion shrinkage and radial lens distortion, are then in the proper preprocessed form as partial input to a simultaneous block triangulation program to be described.

To achieve this objective COMCORDCON utilizes in this case negatives or diapositive plates from a calibrated HASSELBLAD camera equipped with a focal plane reseau grid and nominal 60.0 millimeter focal length lens; the Zeiss, PSK, Precision Stereocomparator augmented by an ancillary IBM 026 card punch; and the OSU, IBM 360/75 computer using a FORTRAN IV G, Level 18 Compiler. Comparable systems may be substituted with necessary modification of data format to provide compatibility.

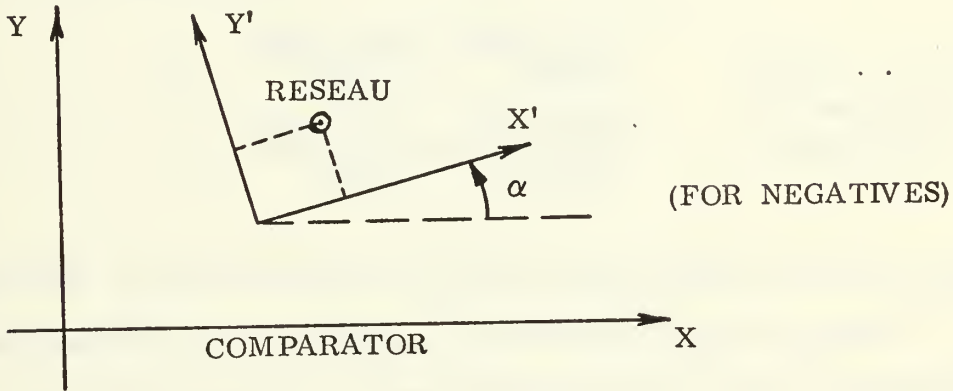
Input consists of the number and interval spacing of the reseau marks on the focal plane grid; the type and identification of the plates; lens distortion values; the coordinates of the center crosses, the object space points, and four neighboring reseau marks (preferably surrounding the object space point); and other job keeping information. This information is then provided to the SUBROUTINES TRANCP and RADIS 1.

TRANCP performs an affine transformation by solving the transformation parameters for each set of four observed reseau marks associated with an image point by a least squares adjustment. These transformation parameters are then employed to obtain the photo coordinates of the image point, corrected for film shrinkage, in the reseau coordinate system of the photograph. The mathematical formulation for this transformation is, for

example:

Assumptions 1. Reseau interval is exactly 10 mm.

2. No correlation between observations of unique points and no correlation between measurements of x and y coordinates in an image point observation.



$$X = A_0 + A_1 X' + A_2 Y'$$

$$Y = B_0 + B_1 X' + B_2 Y'$$

$$F_x = X - A_0 - A_1 X' - A_2 Y' = 0$$

$$F_y = Y - B_0 - B_1 X' - B_2 Y' = 0$$

$$B_X = \left[\frac{\partial F_x}{\partial A} \right] = \begin{bmatrix} -1 & -X_1^1 & -Y_1^1 \\ -1 & -X_2^1 & -Y_2^1 \\ -1 & -X_3^1 & -Y_3^1 \\ -1 & -X_4^1 & -Y_4^1 \end{bmatrix}$$

$$B_Y = \left[\frac{\partial F_y}{\partial B} \right]$$

$$E_X = \begin{bmatrix} F_x \end{bmatrix}_{OBS} = \begin{bmatrix} F_{x1} \\ F_{x2} \\ F_{x3} \\ F_{x4} \end{bmatrix}$$

$$E_Y = \begin{bmatrix} F_y \end{bmatrix}_{OBS}$$

$$W = I; \quad C = B^T B; \quad UX = B^T E_X; \quad UY = B^T E_Y$$

$$\text{PARX} = -\bar{C}^{-1} \text{UX}$$

$$\text{PARY} = -\bar{C}^{-1} \text{UY}$$

$$\text{A} = \text{A} + \text{PARX}$$

$$\text{B} = \text{B} + \text{PARY}$$

The image photo coordinates corrected for film shrinkage in the reseau coordinate system are then:

$$\text{X}' = \frac{\text{A2} (\text{Y} - \text{B0}) - \text{B2} (\text{X} - \text{A0})}{\text{A2 B1} - \text{A1 B2}}$$

$$\text{Y}' = \frac{\text{B1} (\text{X} - \text{A0}) - \text{A1} (\text{Y} - \text{B0})}{\text{A2 B1} - \text{A1 B2}}$$

[Where X and Y are the average of four observations.]

Assumption No. 1 is not necessary since the reseau marks can be measured individually and their true coordinates read into the program [17]. The standard error of their position can be determined and propagated through the complete system if desired.

Assumption No. 2, though not entirely true, can be minimized by careful attention to proper observation techniques.

Both assumptions are made for the sake of simplicity.

SUBROUTINE RADIS 1 employs the current image coordinates and applies a suitable correction based on camera calibration data for radial distortion as a function of the radial distance from the center cross. It assumes a symmetric radial distortion and that the center cross is coincident with the principle point on the plate [17]. Again those assumptions are made for the sake of simplicity. It would be entirely reasonable to integrate into RADIS 1 a correction for the deviation of the center cross from the principle point, a model for non-symmetric radial distortion or a thin prism model for correction of decentering and radial distortion [11] [10].

COMCORDCON supplements its output of corrected photo coordinates by providing the unit standard error of image position after the affine transformation and the standard error of mean of X and Y observations on each object space point observed.

COMCORDCOM

LIST OF PERTINENT VARIABLES AND INPUT DATA

<u>Card No.</u>	<u>Variable</u>	<u>Purpose</u>
	CR	True Reseau Coordinates
	A, B	Transformation Parameters
1	INFO (1)	Job Identification Number
	INFO (2)	Reseau Interval (in microns)
2	CC (1)	X coordinate of left plate center cross (mm)
	CC (2)	Y coordinate of left plate center cross (mm)
	CC (3)	X coordinate of right plate center cross (mm)
	CC (4)	Y coordinate of right plate center cross (mm)
	COND	Defines the plate (s) being used, (RIGHT, LEFT, or BOTH)
	TYPE	Defines the type of plate, (POSITIVE OR NEGATIVE)
	INFO (4)	Left plate photo-identification number
	INFO (5)	Right plate photo-identification number
3	CCO (1)	Point Number
	(2)	Point X Coordinate, Left plate
	(3)	Point Y Coordinate, Left plate
	(4)	Point X Coordinate, Right plate
	(5)	Point Y Coordinate, Right plate
	(6)	Blank
	(7)	Point Number
	(8)	X Coordinate, Upper Left Reseau(#1) Left plate
	(9)	Y Coordinate, Upper Left Reseau(#1) Left plate
	(10)	X Coordinate, Upper Left Reseau(#1) Right plate
	(11)	Y Coordinate, Upper Left Reseau(#1) Right plate
	(12)	Blank

Card No.

- 4 Repeat Observations of Card #3 but Observing Upper Right Reseau (#2)
- 5 Repeat Observations of Card #3 but Observing Lower Right Reseau (#3)
- 6 Repeat Observations of Card #3 but Observing Lower Left Reseau (#4)

The set of cards (3, 4, 5, 6) is repetitive by N number points.


```

0001      COMCORDCON
0002      IMPLICIT REAL*8 (A-H,(-))
0003      DIMENSION CR(5,5,2),CCC(50,4,12),CP(50,14),CC(14)
0004      REAL*8 COND,FIPAGE(14)
0005      INTEGER INFO(5),END,INDEX(4)
0006      NPOINT=0
0007      DO 5 I=1,5
0008      DO 5 J=1,5
0009      CR(I,J,1)=-30.C+FLCAT(J)*10.C
0010      CR(I,J,2)=30.0+FLCAT(1)*10.0
0011      15 READ(5,1001) (INFC(I),I=1,2)
0012      1001 FORMAT(34X,15,35X,15)
0013      20 READ(5,1002) ICC(1),I=1,4),COND,TYPE,(INFC(I),I=4,5)
0014      1002 FORMAT(5X,4(1X,F6.3),1X,A8,1X,A8,2(1X,15))
0015      25 NPOINT=NPOINT+1
0016      DO 30 I=1,4
0017      1000 FORMAT(F4.C,1X,4(1X,F6.3),2(1X,F5.0),4(1X,F6.3),1X,F5.0)
0018      READ(5,1000,END=40) (CCU(NPOINT,I,K),K=1,12)
0019      C
0020      C      TEST FOR END OF DATA
0021      C      TEST TYPE OF INPUT
0022      C
0023      IF ICCU(NPOINT,1,6).NE.C.0) GO TO 35
0024      30 CONTINUE
0025      GO TO 25
0026      35 INFO(3)=NPOINT-1
0027      L=INFO(3)
0028      CALL TRANCP(INFO,CCU,CP,CR,CC,COND,TYPE)
0029      IF (END.NE.C) GO TO 100
0030      INFC(1)=CCU(NPOINT,1,6)
0031      INFC(2)=CCU(NPOINT,1,12)
0032      NPOINT=0
0033      GO TO 20
0034      40 ECC=1
0035      GO TO 35
0036      100 STOP
0037      END

```


TRANCP

```

0001      SUBROUTINE TRANCP(INFC,CCU,CP,CR,CC,CCND,TYPE)
0002      IMPLICIT REAL*8 (A-H,I-Z)
0003      REAL*8 CCND,RIGHT,RIGHT1,RIGHT2,BOTH1,BOTH2,LEFT,LEFT1,LEFT2
0004      DATA PC5/100,
0005      DIMENSION INFO(5),CCU(50,4,12),CP(50,12),B(4,3),EX(4),EY(4),BT(3,4
0006      *,UX(3),UY(3),C(3,3),CR(5,5,2),CC(4),TFORM(4,4),PARX(3),PARY(3)
      INTEGER IUPCS (5)/5,4,3,2,1/

      C
      C      DETERMINE THE PLATE(S) WHOSE COORDINATES ARE TO BE TRANSFORMED
      C      IF CCND=BOTH, BOTH RIGHT AND LEFT COORDINATES WILL BE TRANSFORMED
      C      IF CCND=LEFT, ONLY THE LEFT PLATE COORDINATES WILL BE TRANSFORMED
      C      IF CCND=RIGHT, ONLY THE RIGHT PLATE COORDINATES WILL BE
      C      TRANSFORMED
      C      CCND=LEFT IS ASSUMED AS THE DEFAULT VALUE
      C

0007      INIT=0
0008      IF(CCND.EQ.RIGHT) INIT=2

      C
      C      DETERMINE IF THE PLATE IS POSITIVE OR NEGATIVE
      C      TYPE=NEG IS ASSUMED AS THE DEFAULT VALUE
      C

0009      IDTYPE=2
0010      IF(TYPE.EQ.POS) IDTYPE=1
0011      NPCINT=INFO(3)
0012      RI=INFC(2)/10**3
0013      JPCINT=0
0014      ICCMP=0
0015      N=1
0016      10 JPCINT=JPCINT+1
0017      15 IF(JPCINT.GT.NPCINT) GO TO 200

      C
      C      ESTABLISH A TEMPORARY ARRAY CONTAINING THE COORDINATES OF THE
      C      POINT TO BE TRANSFORMED INTO THE RESFAU SYSTEM
      C

0018      DO 20 I=1,4
0019      TFORM(I,1)=CCU(JPCINT,I,INIT+2)
0020      TFORM(I,2)=CCU(JPCINT,I,INIT+3)
0021      TFORM(I,3)=CCU(JPCINT,I,INIT+8)
0022      20 TFORM(I,4)=CCU(JPCINT,I,INIT+9)
0023      K1=INIT+1
0024      K2=INIT+2

      C
      C      COMPUTE THE RESFAU IDENTIFICATION NUMBER AND ESTABLISH THE CR MATRIX
      C

0025      AC=CC(K1)
0026      BC=CC(K2)
0027      A1=1.0
0028      A2=C.0
0029      B1=0.0
0030      B2=1.0
0031      SUMX=0.0
0032      SUMY=0.0
0033      25 DO 100 J=1,4
0034      ID1=(20.C+TFORM(J,3)-CC(K1))/RI+1.5
0035      ID2=(20.0-TFORM(J,4)+CC(K2))/RI+1.5

      C
      C      IF NECESSARY, CONVERT TO THE POSITIVE SYSTEM
      C

0036      IF(IDTYPE.EQ.1) (C1=IDPOS(ID1)
0037      CCRX=CR(ID2,ID1,1)*(-1.0)**IDTYPE

      C
      C      COMPUTE VALUES OF X,Y, AND ESTABLISH THE EX AND EY MATRICES
      C      ASSUME THE FOLLOWING INITIAL CONDITIONS
      C      AO=XCC
      C      BO=YCC
      C      A1=B2=1.0
      C      A2=B1=C.0
      C

```



```

0038      X=AC+A1*CORX+A2*CR(102,101,2)
0039      Y=BC+B1*CORX+B2*CR(102,101,2)
0040      EX(J)=TFORM(J,3)-X
0041      EY(J)=TFORM(J,4)-Y
0042      IF(1COMP.EC.1) GO TO 100

      C
      C ESTABLISH THE B MATRIX
      C
0043      B(J,1)=-1.0
0044      B(J,2)=CORX*(-1.0)
0045      B(J,3)=CR(102,101,2)*(-1.0)

      C
      C COMPUTE THE SUM OF THE OBJECT IMAGE COORDINATES
      C
0046      SUMX=SUMX+TFORM(J,1)
0047      SUMY=SUMY+TFORM(J,2)

      C
      C TEST FOR FOURTH RESEAU POINT. IF TRUE CONTINUE. OTHERWISE,
      C RETURN FOR NEXT RESEAU POINT
      C
0048      100 CONTINUE
0049      IF(1COMP.EC.1) GO TO 125

      C
      C COMPUTE THE AVERAGE OF THE OBJECT SPACE IMAGE COORDINATES
      C
0050      XAVG=SUMX/4.0
0051      YAVG=SUMY/4.0

      C
      C TRANSPOSE MATRIX B
      C
0052      CALL DGMTRAH(B,4,3)

      C
      C OBTAIN THE UX AND UY MATRICES, WHERE UX=BTRANS*EX AND UY=BTRANS*EY
      C
0053      CALLDGMPRD(BT,EX,UX,1,4,1)
0054      CALLDGMPRD(BT,EY,UY,1,4,1)

      C
      C COMPUTE C MATRIX
      C
0055      CALLDGMPRD(BT,B,C,3,4,3)

      C
      C COMPUTE INVERSE OF C MATRIX
      C
0056      CALLUMINVC(3,D,PARX,PARY)

      C
      C COMPUTE THE TRANSFORMATION PARAMETERS
      C FROM PAR MATRIX, WHERE PAR=-1.C*CINVR*U
      C
0057      DO 80 I=1,3
0058      DO 80 J=1,3
0059      80 C(I,J)=(-1.C)*C(I,J)
0060      CALLDGMPRD(C,UX,PARX,3,3,1)
0061      CALLDGMPRD(C,UY,PARY,3,3,1)
0062      AC=PARX(1)+A0
0063      A1=PARX(2)+A1
0064      A2=PARX(3)+A2
0065      BC=PARY(1)+B0
0066      B1=PARY(2)+B1
0067      B2=PARY(3)+B2

      C
      C COMPUTE COORDINATES IN RESEAU SYSTEM (XPRIME,YPRIME)
      C
0068      DENCM=A2*B1-A1*B2
0069      TERM1=YAVG-B0
0070      TERM2=XAVG-A0
0071      XPRIME=(A2*TERM1-B2*TERM2)/DENCM
0072      YPRIME=(B1*TERM2-A1*TERM1)/DENCM
0073      CALL RADISI(XPRIME,YPRIME,XP,YP,DISTOR)
0074      K3=6*INJ/2

```



```

C      ESTABLISH CP(J,K) MATRIX, WHERE J=J-TH POINT, AND K=K-TH TERM
C      FOR K=1 CR 7      PHOTO IDENTIFICATION NUMBER
C      FOR K=2 CR 8      POINT IDENTIFICATION NUMBER
C      FOR K=3 CR 9      X PRIME WITH THE RADIAL DISTORTION CORRECTION
C      APPLIED
C      FOR K=4 CR 10     Y PRIME WITH THE RADIAL DISTORTION CORRECTION
C      APPLIED
C      FOR K=5 CR 11     STANDARD UNIT ERROR FOR THE FOUR RESEAS ONLY
C      FOR K=6 CR 12     STANDARD ERROR OF ONE OBSERVATION ON THE OBJECT
C      SPACE POINT
0075      CP(JPOINT,1+K3)=INFO(4+INIT/2)
0076      CP(JPOINT,2+K3)=CCC(JPOINT,1,1)
0077      CP(JPOINT,3+K3)=XP
0078      CP(JPOINT,4+K3)=YP
0079      ICCMP=1
0080      GO TO 25
C
C      COMPUTE STANDARD ERROR - POINT BY POINT
C
0081      125 TEMP=0.0
0082      TEMPI=0.0
0083      DO 150 I=1,4
0084      TEMPI=TEMPI+(IFORM(I,1)-XAVG)**2+(IFORM(I,2)-YAVG)**2
0085      150 TEMP=TEMP+EX(I)**2+EY(I)**2
0086      CP(JPOINT,5+K3)=DSRT(TEMP/2)
0087      CP(JPOINT,6+K3)=DSRT(TEMP/748.0)
0088      ICCMP=C
0089      IF(COND.NE.BOTH) GO TO 10
0090      JPCINT=JPOINT+INIT/2
0091      N=N+1
0092      INIT=INIT+(-1)**N*2
0093      GO TO 15
0094      200 WRITE(6,2004) INFO(1)
0095      2004 FORMAT('I',T52,'JOB NUMBER',I6,'//T17,'PHOTO COORDINATES CORRECTED
*FOR LENS AND FILM DISTORTIONS (ZLISS RAK-AK-15/23 NO. 21 197)',//
*/T50,'UNIT STANDARD ERROR (MM)',I60,'STANDARD ERROR OF MEAN OF X A
*ND Y',/T10,'PHOTO',T18,'POINT',T28,'X (MM)',T39,'Y (MM)',T49,'AFTE
*R AFFINE TRANSFORMATION',T81,'ON THE OBJECT SPACE POINT (MM)',/)
0096      IF(COND.EQ.RIGHT) GO TO 225
0097      WRITE(6,2005) ((CP(I,JJ),JJ=1,6),I=1,NPCINT)
0098      GO 210 I=1,NPCINT
0099      IPHOTO=CP(I,1)
0100      IPCINT=CP(I,2)
0101      TEMP=DSRT(CP(I,5)**2+CP(I,6)**2)
0102      210 PUNCH 3000,IPHOTO,IPPOINT,(CP(I,J),J=3,4),TEMP
0103      3000 FORPAT(215,3F10.4)
0104      225 IF(COND.EQ.LEFT) GO TO 250
0105      WRITE(6,2005) ((CP(I,JJ),JJ=7,12),I=1,NPCINT)
0106      GO 235 I=1,NPCINT
0107      IPHOTO=CP(I,7)
0108      IPCINT=CP(I,8)
0109      235 PUNCH 3000,IPHOTO,IPPOINT,(CP(I,J),J=9,10),TEMP
0110      2005 FORMAT('I10,F6.0,T18,F6.0,T26,F9.4,T37,F9.4,T53,E15.5,T67,E15.5,/T
250 RETURN
END

```


RADIS1

C001	SUBROUTINE RADIS1(XP,YP,XP2,YP2,DISTOR)
C002	IMPLICIT REAL*8 (A-H,G-Z)
C003	REAL DISAVG(16)/0.0,0.0,0.0,0.0,0.0,0.0,0.0,0.0,0.0,0.0,0.0,0.0,0.0,0.0,0.0,0.0,
	10.0,0.0,0.0,0.0/
C004	RAD=DSQRT(XP**2+YP**2)
C005	IF(RAD.NE.0.0) GO TO 10
C006	DISTOR=0.0
C007	RETURN
C008	10 K=RAD/10.0*1.0
C009	DISTOR=DISAVG(K)/10**3
C010	XP2=XP-DISTOR*XP/RAD
C011	YP2=YP-DISTOR*YP/RAD
C012	RETURN
C013	END

*** SAMPLE DATA COMCORDCON ***

1 LEFT		NEG			
70 90	0 00 00 0	00 00 00			
01	- 23 72 7	1 22 41	01	- 20 00 0	0 00 00
01	- 23 72 5	1 22 39	01	- 99 9 8	- 00 06
01	- 23 72 5	1 22 41	01	- 99 9 0	- 99 91
01	- 23 72 1	1 22 40	01	- 19 99 3	- 99 93
02	6 95 0	6 32	02	00 00 1	- 00 05
02	6 95 4	6 36	02	99 9 8	- 00 04
02	6 95 0	6 39	02	10 00 5	- 99 96
02	6 95 0	6 37	02	00 8	- 99 93
04	- 0 02 1	74 52	04	00 0	- 00 09
04	- 0 02 2	74 52	04	99 9 7	00 00
04	- 0 02 7	74 46	04	10 00 6	- 99 92
04	- 0 02 0	74 44	04	00 0 9	- 99 93
05	10 83 0	72 26	05	99 9 9	- 00 05
05	10 83 0	72 26	05	20 00 0	00 00
05	10 83 4	72 25	05	20 00 7	- 99 93
05	10 83 7	72 25	05	10 00 9	- 99 96

APPENDIX II

BLOCK TRIANGULATION PROGRAM

The Block Triangulation Program performs a spatial resection and orientation by a simultaneous least squares adjustment treating photo and survey coordinates and the elements of exterior orientation as observed quantities. As significant input it utilizes values of the camera constant (focal length); corrected photo coordinates output from COMORDCON; observed values of exterior orientation equated to the initial approximations; and various job keeping information such as number of photographs, number of unique points, photograph number, etc. Additionally, variance-covariance matrices are estimated and input to the program for the photo coordinates, survey coordinates, and the elements of exterior orientation.

The simplifying assumption that there is no correlation between photo coordinates, survey coordinates, and the elements of exterior orientation is employed. It is further assumed that no significant correlation exists between the individual survey coordinates, the individual elements of exterior orientation and individual photographs.

The output of this program provides the minimum variance solution for the adjusted values of the elements of exterior orientation and the survey coordinates.

This solution is effected through the following mathematical formulation:

The observation equations are :

$$\begin{aligned} \overset{\circ}{V} + \overset{\circ}{B} \overset{\circ}{\Delta} + \overset{s}{B} \overset{s}{\Delta} + \epsilon &= 0 \\ \overset{\circ}{V} - \overset{\circ}{\Delta} + \epsilon &= 0 \\ \overset{s}{V} - \overset{s}{\Delta} + \epsilon &= 0 \end{aligned}$$

In matrix form

$$\begin{bmatrix} \overset{\circ}{V} \\ \overset{s}{V} \end{bmatrix} + \begin{bmatrix} \overset{\circ}{B} & \overset{s}{B} \\ -I & 0 \\ 0 & -I \end{bmatrix} \begin{bmatrix} \overset{\circ}{\Delta} \\ \overset{s}{\Delta} \end{bmatrix} + \begin{bmatrix} \epsilon \\ \overset{\circ}{\epsilon} \\ \overset{s}{\epsilon} \\ \epsilon \end{bmatrix} = 0$$

or,

$$\bar{V} + \bar{B} \bar{\Delta} + \bar{\epsilon} = 0$$

Then by exercising the method of LAGRANGE for realizing the minimum variance solution we have:

$$F = \bar{V}^T \bar{W} \bar{V} - 2\lambda^T (\bar{V} + \bar{B} \bar{\Delta} + \bar{\epsilon})$$

$$\text{and, } \left[\frac{\partial F}{\partial \bar{V}} \right] = 0$$

$$\left[\frac{\partial F}{\partial \bar{\lambda}} \right] = 0$$

$$\left[\frac{\partial F}{\partial \bar{\Delta}} \right] = 0$$

thus

$$(B^T W B) \Delta + (B W \epsilon) = 0$$

EQUATION A

where

$$\bar{B} = \begin{bmatrix} \overset{\circ}{B} & \overset{s}{B} \end{bmatrix}; \quad \overset{\circ}{B} = \begin{bmatrix} \overset{\circ}{B}_1 & \overset{\circ}{B}_2 & \dots & 0 \\ 0 & \dots & \dots & \overset{\circ}{B}_{3n} \end{bmatrix}; \quad \overset{\circ}{B}_j = \begin{bmatrix} \frac{\partial X_j}{\partial (X_0, Y_0, Z_0, \kappa_0, \varphi_0, \omega_0)} \\ \frac{\partial Y_j}{\partial (X_0, Y_0, Z_0, \kappa_0, \varphi_0, \omega_0)} \end{bmatrix}$$

$$\overset{s}{B} = \begin{bmatrix} \overset{s}{B}_1 & \overset{s}{B}_2 & \dots & 0 \\ 0 & \dots & \dots & \overset{s}{B}_{3n} \end{bmatrix}; \quad \overset{s}{B}_j = \begin{bmatrix} \frac{\partial X_j}{\partial (X, Y, Z)} \\ \frac{\partial Y_j}{\partial (X, Y, Z)} \end{bmatrix}$$

$$\bar{W} = \begin{bmatrix} W & \overset{\circ}{W} & 0 \\ 0 & W & \overset{s}{W} \end{bmatrix}; \quad W = \begin{bmatrix} W_1 & W_2 & 0 \\ 0 & \ddots & W_{2n} \end{bmatrix}; \quad W_j = \begin{bmatrix} W_{xx} & 0 \\ 0 & W_{yy} \end{bmatrix}$$

$$\overset{\circ}{W} = \begin{bmatrix} \overset{\circ}{W}_1 & \overset{\circ}{W}_2 & 0 \\ 0 & \ddots & \overset{\circ}{W}_m \end{bmatrix}; \quad \overset{\circ}{W}_j = \begin{bmatrix} W_{x_0 x_0} & W_{y_0 y_0} & 0 \\ 0 & W_{\omega_0 \omega_0} & \end{bmatrix}$$

$$\overset{s}{W} = \begin{bmatrix} \overset{s}{W}_1 & \overset{s}{W}_2 & 0 \\ 0 & \ddots & \overset{s}{W}_n \end{bmatrix}; \quad \overset{s}{W}_j = \begin{bmatrix} W_{xx} & W_{yy} & 0 \\ 0 & W_{zz} & \end{bmatrix}$$

$$\bar{\Delta} = \begin{bmatrix} \overset{\circ}{\Delta} \\ \overset{s}{\Delta} \end{bmatrix}; \quad \overset{\circ}{\Delta} = \begin{bmatrix} \overset{\circ}{\delta}_1 \\ \overset{\circ}{\delta}_2 \\ \vdots \\ \overset{\circ}{\delta}_m \end{bmatrix}; \quad \epsilon = \begin{bmatrix} \overset{\circ}{\delta}_1 \\ \overset{\circ}{\delta}_2 \\ \vdots \\ \overset{\circ}{\delta}_{3n} \end{bmatrix}; \quad \overset{s}{\Delta} = \begin{bmatrix} \overset{s}{\delta}_1 \\ \overset{s}{\delta}_2 \\ \vdots \\ \overset{s}{\delta}_{3n} \end{bmatrix}; \quad \delta_j = \begin{bmatrix} \delta X_j \\ \delta Y_j \\ \delta Z_j \end{bmatrix}$$

$$\bar{\epsilon} = \begin{bmatrix} \epsilon \\ \overset{\circ}{\epsilon} \\ \overset{s}{\epsilon} \end{bmatrix}; \quad \epsilon = \begin{bmatrix} x_1^0 - \overset{\infty}{x}_1 \\ y_1^0 - \overset{\infty}{y}_1 \\ y_n^0 - \overset{\infty}{y}_n \end{bmatrix}; \quad \overset{\circ}{\epsilon} = \begin{bmatrix} \overset{\circ}{X}_1 - \overset{\infty}{X}_1 \\ \overset{\circ}{Y}_1 - \overset{\infty}{Y}_1 \\ \vdots \\ \overset{\circ}{\omega}_1 - \overset{\infty}{\omega}_1 \\ \vdots \\ \overset{\circ}{\omega}_{6m} - \overset{\infty}{\omega}_{6m} \end{bmatrix}$$

$$\overset{s}{\epsilon} = \begin{bmatrix} \overset{s}{X}_1 - \overset{\infty}{X}_1 \\ \overset{s}{Y}_1 - \overset{\infty}{Y}_1 \\ \overset{s}{Z}_1 - \overset{\infty}{Z}_1 \\ \vdots \\ \overset{s}{Z}_{3n} - \overset{\infty}{Z}_{3n} \end{bmatrix}$$

$$\bar{B} \bar{W} \bar{\epsilon} = \bar{U} = \begin{bmatrix} U_1 \\ U_2 \end{bmatrix}; \quad U_1 = \overset{\circ}{B}^T \overset{\circ}{W} \overset{\circ}{\epsilon} - \overset{\circ}{W} \overset{\circ}{\epsilon}$$

$$U_2 = \overset{s}{B}^T \overset{s}{W} \overset{s}{\epsilon} - \overset{s}{W} \overset{s}{\epsilon}$$

with m = the number of photos and n = the number of unique points.

Expanding EQUATION A provides;

$$\begin{bmatrix} \overset{\circ}{B}^T - I & 0 \\ \overset{s}{B}^T & 0 - I \end{bmatrix} \begin{bmatrix} \overset{\circ}{W} & \overset{\circ}{0} \\ 0 & \overset{s}{W} \end{bmatrix} \begin{bmatrix} \overset{\circ}{B} & \overset{s}{B} \\ -I & 0 \\ 0 & -I \end{bmatrix} \begin{bmatrix} \overset{\circ}{\Delta} \\ \overset{s}{\Delta} \end{bmatrix} + \begin{bmatrix} \overset{\circ}{B}^T - I & 0 \\ \overset{s}{B}^T & 0 - I \end{bmatrix} \begin{bmatrix} \overset{\circ}{W} & \overset{\circ}{0} \\ 0 & \overset{s}{W} \end{bmatrix} \begin{bmatrix} \epsilon \\ \overset{\circ}{\epsilon} \\ \overset{s}{\epsilon} \\ \epsilon \end{bmatrix} = 0$$

and after multiplying out,

$$\left[\begin{array}{c|c} \overset{\circ}{B}^T \overset{\circ}{W} \overset{\circ}{B} + \overset{\circ}{W} & \overset{\circ}{B}^T \overset{\circ}{W} \overset{s}{B} \\ \hline \overset{s}{B}^T \overset{\circ}{W} \overset{\circ}{B} & \overset{s}{B}^T \overset{\circ}{W} \overset{s}{B} + \overset{s}{W} \end{array} \right] \begin{bmatrix} \overset{\circ}{\Delta} \\ \overset{s}{\Delta} \end{bmatrix} + \begin{bmatrix} \overset{\circ}{B}^T \overset{\circ}{W} \epsilon - \overset{\circ}{W} \epsilon \\ \overset{s}{B}^T \overset{\circ}{W} \epsilon - \overset{s}{W} \epsilon \end{bmatrix} = 0 \quad \text{EQUATION B}$$

$$\text{and } \bar{N} \bar{\Delta} + \bar{U} = 0$$

By inspection one can ascertain that $\overset{\circ}{B}^T \overset{\circ}{W} \overset{\circ}{B} + \overset{\circ}{W}$ is a full six by six matrix with one photo, but for m photos, a block diagonal matrix of 6 m by 6 m consisting of six by six submatrices. Analogously, $\overset{\circ}{B}^T \overset{\circ}{W} \overset{s}{B}$ and $\overset{s}{B}^T \overset{\circ}{W} \overset{\circ}{B}$ will be 6 by 3 n and 3 n by 6 respectively for one photo but 6 m by 3 n and 3 n by 6 m for m photos. $\overset{s}{B}^T \overset{s}{W} \overset{s}{B} + \overset{s}{W}$ will naturally be 3 n by 3 n for one or m photos. However, because of the assumption that there was no correlation in W and $\overset{s}{W}$, $\overset{s}{B}^T \overset{s}{W} \overset{s}{B} + \overset{s}{W}$ is a block diagonal matrix of three by three submatrices. These facts concerning this system of normal equations lend EQUATION B to a simplified method of inversion by partitioning [13].

$$\bar{N} = \left[\begin{array}{c|c} \overset{\circ}{B}^T \overset{\circ}{W} \overset{\circ}{B} + \overset{\circ}{W} & \overset{\circ}{B}^T \overset{\circ}{W} \overset{s}{B} \\ \hline \overset{s}{B}^T \overset{\circ}{W} \overset{\circ}{B} & \overset{s}{B}^T \overset{\circ}{W} \overset{s}{B} + \overset{s}{W} \end{array} \right] = \left[\begin{array}{c|c} A & B \\ \hline C & D \end{array} \right]$$

where \bar{N} is of the rth order and A and D are of order 6 m and 3 n respectively;
 $r = 6 m + 3 n$

$$\bar{N}^{-1} = \left[\begin{array}{c|c} K & L \\ \hline M & N \end{array} \right] \quad \text{and} \quad \bar{N}^{-1} \bar{N} = I$$

therefore

$$A K + B M = I$$

$$A L + B N = 0$$

$$C K + D M = 0$$

$$C L + D N = I$$

It can then be verified that;

$$K = (A - B D^{-1} C)^{-1}$$

$$L = K B D^{-1}$$

$$M = -D^{-1} C K$$

$$N = D^{-1} - D^{-1} C L$$

thus;

$$\bar{N}^{-1} = \left[\begin{array}{c|c} (A - B D^{-1} C)^{-1} & K B D^{-1} \\ \hline -D^{-1} C K & D^{-1} - D^{-1} C L \end{array} \right]$$

and where $\overset{\circ}{N} = \overset{\circ}{B}^T \overset{\circ}{W} \overset{\circ}{B}$; $\overset{s}{N} = \overset{s}{B}^T \overset{s}{W} \overset{s}{B}$; $\overset{c}{N} = \overset{c}{B}^T \overset{s}{W} \overset{s}{B}$

$$\bar{N}^{-1} = \left[\begin{array}{c|c} (\overset{\circ}{N} + \overset{\circ}{W}) - \overset{c}{N}(\overset{s}{N} + \overset{s}{W})^{-1} \overset{c}{N}^T & -\overset{c}{K} \overset{c}{N}(\overset{s}{N} + \overset{s}{W})^{-1} \\ \hline -(\overset{s}{N} + \overset{s}{W})^{-1} \overset{c}{N}^T \overset{c}{K} & (\overset{s}{N} + \overset{s}{W})^{-1} - (\overset{s}{N} + \overset{s}{W})^{-1} \overset{c}{N}^T \overset{c}{L} \end{array} \right]$$

As a result only one 6 m by 6 m matrix, and n three by three matrices must be inverted in the partitioned matrix to effect the inversion of \bar{N} , an rth order square matrix ($r = 6m + 3n$), for m photos and n unique points. In solving the normal equations the solution then to the alterations to current approximations is: $\bar{\Delta} = -\bar{N}^{-1} U$ and the adjusted solution vector is computed as;

$$X_a = \overset{\infty}{X} + \bar{\Delta}$$

with subsequent iteration converging to a suitable solution.

$$X_{a_{i+1}} = X_{a_i} + \bar{\Delta}_i$$

The BLOCK TRIANGULATION PROGRAM is capable of processing up to twelve photographs, 36 unique points, and a selected number of iterations with but minor modifications. Additionally, it provides the standard error of

unit weight, and the residuals, standard error, and the variance-covariance matrices of adjusted parameters.

Other than standard library subroutines this program utilizes SUBROUTINES MATINV and COFEI. MATINV is merely a double precision; matrix inversion routine employing a bordering technique; COFEI computes the partial derivatives of the projective equations with respect to the elements of exterior orientation. The main program provides for updating photograph and point information for use on successive passes of the iterative process.

The terms in the preceding discussion are defined as:

V = residuals on observations

B = partial derivatives of the projective equations

Δ, δ = alterations to current estimate of the unknowns

ϵ = functional relationship between the observations and
unknowns evaluated at the current estimates

λ = Lagrange multiplier

W = weight matrix

x, y = photo coordinates

X, Y, Z = survey coordinates

$X_o, Y_o, Z_o,$
 κ, φ, ω = elements of exterior orientation

Superscripts

^e; refers to elements of exterior orientation

^s; refers to survey system

none; refers to photo system

^o; refers to observed values

[∞]; refers to computed values using approximations to unknowns

BLOCK TRIANGULATION
LIST OF PERTINENT VARIABLES AND INPUT DATA

<u>CARD NO.</u>	<u>VARIABLE</u>	<u>PURPOSE</u>
	A	Elements of \bar{N} and \bar{N}^{-1}
	U1, U2	Constant vector
	DE	Alterations to elements of exterior orientation
	DS	Alterations to survey coordinates
	E	Residuals on x, y photo coordinates
	R	$\sin(\kappa, \phi, \omega) \cos(\kappa, \phi, \omega)$
1	CC	Camera constant (f in mm)
	N	Number of photographs
2	WM	A scalar multiplier of a 2 by 2 identity matrix (I) to provide an estimated variance-covariance matrix for observations on photo-point coordinates
	IP	Total number of unique points
3	Photo(1, 1)	Number of points in photograph
4, 5, 6, 7, 8, 9	Photo(1, 2-7) [X0, EE]	Current approximation and observed values (equated) of the elements of exterior orientation (m, and radians)
10, 11, 12, 13, 14, 15	Photo(1, 14-19)	Estimated variance-covariance matrix for exterior orientation
16	Photo(1, 1, 1-2)	x, y photo coordinates (COMCORDCON)
17	Photo(1, 1, 3)	Point number
18, 19, 20	Point(1, 1, 17-22) (X, ES)	Current approximation and observed values (equated) of survey coordinates (m)
21, 22, 23	Point(1, 1, 8-10)	Estimated variance-covariance matrix for survey coordinates

CARDS 3 through 15 repeat by m number of photographs and 16 through 23 repeat by n number of points in each photograph.

MAIN

[illegible]


```

C CALL PHOTO DATA
C
0064 TPC=1
0065 DO 100 J=1,N
0066 LOC=13
0067 K=PHOTO(J,1)
0068 DO 210 II=2,7
0069 XG(II-1)=PHOTO(J,II)
0070 EE(II-1)=PHOTO(J,II+6)
0071 DO 210 JJ=1,6
0072 LOC=LOC+1
0073 210 WF(II-1,JJ)=PHOTO(J,LOC)
0074 WRITE(6,601) XC
0075 WRITE(6,601) EE
0076 601 FORMAT(6E15.5,/(6E15.5))
0077 R(1)=DSIN(X014)
0078 R(2)=DSIN(X015)
0079 R(3)=DSIN(X016)
0080 R(4)=DCOS(X014)
0081 R(5)=DCOS(X015)
0082 R(6)=DCOS(X016)

C
C ADDING TERMS DUE TO CONSTRAINTS ON EXTERIOR ORIENTATION ELEMENTS
C
0083 L=0*(J-1)
0084 DO 10 II=1,6
0085 IF(WE(II,11)-NE(0,0)) DF=DF+1.0
0086 VDF=VDF+WE(II,11)*(EE(11)-X0(11))**2
0087 DO 10 JJ=1,6
0088 U(II+11)=01(L+11)-WE(II,JJ)*EE(JJ)-X0(JJ)
0089 10 A11(L+11,L+JJ)=A11(L+11,L+JJ)+WE(II,JJ)

C
C CALL POINT DATA
C
0090 DO 100 I=1,K
0091 DATA11=POINT(J,I,1)
0092 DATA12=POINT(J,I,2)
0093 P=POINT(J,I,3)
0094 LOC=3
0095 DO 215 II=1,2
0096 DO 215 JJ=1,2
0097 LOC=LOC+1
0098 215 W(II,JJ)=POINT(J,I,LOC)
0099 DO 216 II=1,3
0100 DO 216 JJ=1,3
0101 LOC=LOC+1
0102 216 WS(II,JJ)=POINT(J,I,LOC)
0103 DO 217 II=17,19
0104 X(II-16)=POINT(J,I,II)
0105 217 ES(II-16)=POINT(J,I,II+3)
0106 WRITE(6,601) X
0107 WRITE(6,601) ES
0108 DF=DF+2.0
0109 LL=3*(P-1)

C
C CALL PARTIALS
C
0110 CALL CCFET(X,R,B,X0,CC,XC,YC)

C
C COMPUTE NORMALS
0111 ITEST=1
0112 IF(KEY(P).GT.0) GO TO 12
0113 KEY(P)=P
0114 ITEST=0
0115 12 DO 15 II=1,6
0116 DO 15 JJ=1,2
0117 ATEMP(II,JJ)=0.0
0118 DO 15 KK=1,2
0119 15 ATEMP(II,JJ)=ATEMP(II,JJ)+B(KK,II)*W(KK,JJ)
0120 E(1)=DATA11-XC
0121 E(2)=DATA12-YC
0122 VDF=VDF+W(1,1)*E(1)**2+W(2,2)*E(2)**2

```



```

C      COMPUTE A11
0123      DO 17 I1=1,6
0124      DO 16 KK=1,2
0125      16 C1(L+I1)=C1(L+I1)+ATEMP(I1,KK)*E(KK)
0126      DO 17 JJ=1,6
0127      DO 17 KK=1,2
0128      17 A11(L+I1,L+JJ)=A11(L+I1,L+JJ)+ATEMP(I1,KK)*B(KK,JJ)

C
C      COMPUTE A12
0129      DO 19 I1=1,6
0130      DO 19 JJ=7,9
0131      DO 19 KK=1,2
0132      19 A12(L+I1,LL+JJ-6)=A12(L+I1,LL+JJ-6)+ATEMP(I1,KK)*B(KK,JJ)

C
C      COMPUTE A21
C
C      COMPUTE A22
0133      DO 23 I1=7,9
0134      DO 23 JJ=1,2
0135      ATEMP(I1-6,JJ)=0.0
0136      DO 23 KK=1,2
0137      23 ATEMP(I1-6,JJ)=ATEMP(I1-6,JJ)+B(KK,I1)*W(KK,JJ)
0138      DO 27 I1=1,3
0139      M=LL+I1
0140      DO 26 KK=1,2
0141      U2(M)=U2(M)+ATEMP(I1,KK)*E(KK)
0142      DO 26 JJ=7,9
0143      26 A22(M,LL+JJ-6)=A22(M,LL+JJ-6)+ATEMP(I1,KK)*B(KK,JJ)
0144      IF(I1.EQ.1) GO TO 27

C
C      ADDING TERMS DUE TO CONSTRAINT ON SURVEY COORDINATES
0145      VDF=VDF+WS(I1,I1)*(ES(I1)-X(I1))**2
0146      IF(WS(I1,I1).NE.0.0) DF=DF+1.0
0147      DO 28 JJ=1,3
0148      A22(M,LL+JJ)=A22(M,LL+JJ)+WS(I1,JJ)
0149      28 U2(M)=U2(M)-WS(I1,JJ)*(ES(I1)-X(I1))
0150      27 CONTINUE
0151      100 CONTINUE
0152      IF(1001.EQ.1) GO TO 300

C
C      FORMING B11
C
0153      CALL MATINV(A22,K1)
0154      DO 35 I=1,K1
0155      DO 35 J=1,J1
0156      A22T(I,J)=0.0
0157      DO 35 K=1,K1
0158      35 A22T(I,J)=A22T(I,J)+A22(I,K)*A12(J,K)
0159      DO 36 I=1,J1
0160      DO 36 J=1,J1
0161      DO 36 K=1,K1
0162      36 A11(I,J)=A11(I,J)-A12(I,K)*A22T(K,J)
0163      CALL MATINV(A11,J1)

C
C      FORMING B12
C
0164      DO 37 I=1,J1
0165      DO 37 J=1,K1
0166      B12T(I,J)=0.0
0167      DO 37 K=1,K1
0168      37 B12T(I,J)=B12T(I,J)+A12(I,K)*A22(K,J)
0169      DO 38 I=1,J1
0170      DO 38 J=1,K1
0171      A12(I,J)=0.0
0172      DO 38 K=1,K1
0173      38 A12(I,J)=A12(I,J)-A11(I,K)*B12T(K,J)

```



```

      C      FORMING B22
      C
0174      DO 39 I=1,K1
0175      DO 39 J=1,K1
0176      DO 39 K=1,J1
0177      39 A22(I,J)=A22(I,J)-A22(I,K)*A12(K,J)

      C
      C      SOLVING NORMALS
      C
0178      DO 40 I=1,J1
0179      DE(I)=0.0
0180      DO 41 J=1,J1
0181      41 DE(I)=DE(I)-A11(I,J)*U1(J)
0182      DO 40 J=1,K1
0183      40 DE(I)=DE(I)-A12(I,J)*U2(J)
0184      DO 42 I=1,K1
0185      DS(I)=0.0
0186      DO 43 J=1,K1
0187      43 DS(I)=DS(I)-A22(I,J)*U2(J)
0188      DO 42 J=1,J1
0189      42 DS(I)=DS(I)-A12(J,I)*U1(J)

      C
      C      APPLY ALTERATIONS
      C
0190      DO 115 I=1,N
0191      K=PHOTO(I,1)
0192      DO 101 IZ=2,7
0193      PHOTO(I,IZ)=PHOTO(I,IZ)+DE(6*(I-1)+IZ-1)
0194      101 CONTINUE
0195      DO 115 J=1,K
0196      P=POINT(I,J,3)
0197      DO 115 IZ=17,19
0198      POINT(I,J,IZ)=POINT(I,J,IZ)+DS(3*(P-1)+IZ-16)
0199      115 CONTINUE
0200      IF(1/CYCLE,LT.8) GO TO 4
0201      DF=0.0
0202      VDF=C.0
0203      IOUT=1
0204      GO TO 4
0205      300 CALL MATINV(A11,J1)
0206      CALL MATINV(A22,K1)
0207      DF=LF-J1-K1
0208      VAR=VDF/DF
0209      UNSTOR=DSORT(VAR)
0210      CALL IOATIME(1YEAR,1MONTH,1DAY,1TIME)
0211      DO 306 I=1,J1
0212      DO 306 J=1,J1
0213      306 A11(I,J)=A11(I,J)*VAR
0214      DO 307 I=1,K1
0215      DO 307 J=1,K1
0216      307 A22(I,J)=A22(I,J)*VAR
0217      NDF=DF
0218      DO 301 I=1,24
0219      IF(1TIME,LT.300000) GO TO 302
0220      301 1TIME=1TIME-300000
0221      302 DO 303 J=1,59
0222      IF(1TIME,LT.60000) GO TO 304
0223      303 1TIME=1TIME-60000
0224      304 1IME=FLOAT(1TIME)/100.0
0225      I=I-1
0226      J=J-1
0227      WRITE(6,3000) 1TIME,JOBNUM,1DAY,MONTH(1MONTH),1YEAR,I,J,1TIME,N,NO
      *F,UNSTOR
0228      WRITE(11,3003) WM
0229      WRITE(12,3005)
0230      WRITE(6,3001)
0231      DO 310 I=1,N
0232      16=6*(I-1)
0233      DO 305 J=1,6
0234      XO(J)=DSORT(A11(16+J,16+J))
0235      305 EE(J)=PHOTO(1,J+7)-PHOTO(1,J+1)
0236      WRITE(6,3002) 1,(PHOTO(1,J+1),J=1,6),XO,EE,(PHOTO(1,J),J=14,49,7)

```



```

0237      WRITE(6,3007) ((A11(I6*K,I6+J),J=1,6),K=1,6)
0238      WRITE(6,3007)
0239      R(1)=OSIN(PHOTO(I,5))
0240      R(2)=OSIN(PHOTO(I,6))
0241      R(3)=OSIN(PHOTO(I,7))
0242      R(4)=UCOS(PHOTO(I,5))
0243      R(5)=UCOS(PHOTO(I,6))
0244      R(6)=UCOS(PHOTO(I,7))
0245      K=PHOTO(I,1)
0246      DO 325 J=1,K
0247      P=POINT(I,J,3)
0248      KK=3*(P-1)
0249      DX=POINT(I,J,17)-PHOTO(I,2)
0250      DY=POINT(I,J,18)-PHOTO(I,3)
0251      DZ=POINT(I,J,19)-PHOTO(I,4)
0252      XT=DX*R(5)*R(4)+DY*(R(6)*R(1)+R(3)*R(2)*R(4))+DZ*(R(3)*R(1)-R(6)*
* (2)*R(4))
0253      YT=-DX*(R(5)*R(1)+DY*(R(6)*P(4)-R(3)*R(2)*R(1))+DZ*(R(3)*R(4)+R(6)*
* R(2)*R(1))
0254      ZT=DX*R(2)-DY*R(3)*R(5)+DZ*R(6)*R(5)
0255      XC=CC*XT/ZT
0256      YC=CC*YT/ZT
0257      E(1)=POINT(I,J,1)-XC
0258      E(2)=POINT(I,J,2)-YC
0259      WRITE(1,3004) I,P,POINT(I,J,1),POINT(I,J,2),E(1),E(2)
0260      IF(KEY(P).EQ.0) GO TO 325
0261      KEY(P)=0
0262      DO 320 JJ=1,3
0263      X(JJ)=DSQRT(A22(KK+JJ,KK+JJ))
0264      320 ES(JJ)=POINT(I,J,JJ+19)-POINT(I,J,JJ+16)
0265      WRITE(2,3006) P,(POINT(I,J,JJ),JJ=17,19),X,ES,(POINT(I,J,JJ),JJ=8,
* 16,4)
0266      WRITE(2,3008)((A22(KK+II,KK+JJ),JJ=1,3),II=1,3)
0267      WRITE(2,3009)
0268      IF(J/2*.EQ.J) WRITE(2,3010)
0269      325 CONTINUE
0270      330 CONTINUE
0271      3000 FORMAT('1',26(/),T47,T44,/T53,'JOB NUMBER',16,/T53,'DATE',13,1X,A4
* ,15,/T54,'TIME',13,':',12,':',F4.1,/T51,'NUMBER OF PHOTOS = ',12,/
* 149,'DEGREES OF FREEDOM = ',15,/T44,'UNIT STANDARD ERROR = ',D12.5)
0272      3001 FORMAT('1',T58,'RESULTS',/T51,'EXTERIOR ORIENTATION')
0273      3002 FORMAT(/T10,'PHOTO NO. ',12,T27,'XO (METERS)',T41,'YO (METERS)',
* T57,'ZO (METERS)',T73,'KAPPA (RAD.)',T91,'PHI (RAD.)',T107,'OMEGA
* (RAD.)',/T120,3F16.3,3D17.6,/T9,'STD. ERROR',T20,4D16.4,2(1X,D16.4)
* ,/T9,'RESIDUALS',T20,4D16.4,2(1X,D16.4),/T9,'WEIGHTS',T20,6F16.3
* ,/)
0274      3003 FORMAT(T58,'RESULTS',/T53,'PHOTO COORDINATES',/T47,'(ALL WEIGHTS T
* AKEN AS ',F7.1,')',/T27,'PHOTO NO.',T41,'POINT NO.',T55,'X (MM)',
0274      3004 FORMAT('0',T30,12,T44,13,T50,2F11.3,T73,2D16.4)
0275      3005 FORMAT(T49,'RESULTS',/T52,'SURVEY COORDINATES')
0276      3006 FORMAT(/T31,'POINT NO. ',13,T52,'X',T68,'Y',T84,'Z',/T42,3F16.3,
* /T32,'STD. ERROR',T43,3D16.4,/T32,'RESIDUALS',T43,3D16.4,/T32,'
* WEIGHTS',4X,3F16.3,/)
0277      3007 FORMAT('0',14H,'VARIANCE/COVARIANCE MATRIX',/T16,6E15.5,/)
0278      3008 FORMAT('0',14H,'VARIANCE/COVARIANCE MATRIX',/T36,3E15.5,/)
0279      3009 FORMAT('0',/)
0280      3010 FORMAT('1',/)
0281      500 FORMAT(2F10.5)
0282      501 FORMAT(6F10.5)
0283      502 FORMAT(2F10.4)
0284      503 FORMAT(15)
0285      504 FORMAT(3F10.3)
0286      505 FORMAT('1',PHOTO NUMBER',13)
0287      506 FORMAT('1',POINT NUMBER',14,/)
0288      510 FORMAT(7A4,2X,14)
0289      600 FORMAT(1X,D15.7)
0290      603 FORMAT(F5.0)
0291      STOP
0292      DEBUG SUBCHK
0293      END

```


MATINV

```

0001      SUBROUTINE MATINV(A,N)
0002      IMPLICIT REAL*8(A-H,O-Z)
0003      DIMENSION A(N,N),B(140),C(140)
0004      M=N-1
0005      A(1,1)=1.0/A(1,1)
0006      IF(M) 2900,2906,2900
0007      2900 DO 2905 I=1,M
0008          L=I+1
0009          DO 2901 J=L,I
0010              B(J)=0.0
0011          2901 C(J)=0.0
0012              DO 2902 J=1,I
0013                  DO 2902 K=1,I
0014                      B(J)=B(J)-A(K,J)*A(L,K)
0015          2902 C(K)=C(K)-A(K,J)*A(J,L)
0016              D=A(L,L)
0017              DO 2903 J=1,I
0018                  2903 D=D+C(J)*A(L,J)
0019              D=1.0/D
0020              DO 2904 J=1,I
0021                  A(J,L)=C(J)*D
0022                  A(L,J)=B(J)*D
0023              DO 2904 K=1,I
0024                  A(J,K)=A(J,K)+B(K)*C(J)*D
0025          2905 A(L,L)=D
0026          2906 RETURN
0027      END

```


COFE1

```

0001      SUBROUTINE COFE1(D,R,H,X0,CC,XC,YC)
      C
      C COMPUTES B FOR EXTERIOR AND INTERIOR ELEMENTS INCLUDING CC
      C REQUIRED ORDER (X,Y,Z,K,P,W)
      C NUMBER OF POINT WHOSE COEFFICIENTS ARE BEING CALCULATED
      C CAMERA CONSTANT TAKEN NEGATIVE
      C K= MATRIX(SK,SP,SW,CK,CP,CW)
      C DATA= MATRIX(PT,X,Y,MX,MY,X,Y,Z)
      C
0002      IMPLICIT REAL*8(A-H,O-Z)
0003      DIMENSION R(6),D(3),X0(6),B(2,9)
0004      SK=R(1)
0005      SP=R(2)
0006      SW=R(3)
0007      CK=R(4)
0008      CP=R(5)
0009      CW=R(6)
0010      LX=D(1)-X0(1)
0011      LY=D(2)-X0(2)
0012      LZ=D(3)-X0(3)
0013      CO=110*LEI**6
0014      B(1,1)=0.0
0015      B(2,1)=0.0
0016      XI=DX*CP*CK+DY*(CW*SK+SW*SP*CK)+DZ*(SW*SK-CW*SP*CK)
0017      YT=-DX*CP*SK+DY*(CW*CK-SW*SP*SK)+DZ*(SW*CK+CW*SP*SK)
0018      ZI=DX*SP-DY*SW*CP+DZ*CW*CP
0019      COZ=CO*(1.0/ZI**2)
0020      B(1,1)=-COZ*(ZI*CP*CK-XI*SP)
0021      B(1,2)=-COZ*(ZI*(CW*SK+SW*SP*CK)+XI*SW*CP)
0022      B(1,3)=-COZ*(ZI*(SW*SK-CW*SP*CK)-XI*CW*CP)
0023      B(1,4)=-COZ*(XI*(-DX*CP*SK+DY*(CW*CK-SW*SP*SK)+DZ*(SW*CK+CW*SP*SK)
110      )+ZI
0024      B(1,5)=-COZ*(ZI*(-DX*SP*CK+DY*SW*CP*CK-DZ*CW*CP*CK)-XI*(DX*
      LCP+DY*SW*SP-DZ*CW*SP))
0025      B(1,6)=-COZ*(ZI*(DY*(CW*SP*CK-SW*SK)+DZ*(CW*SK+SW*SP*CK))+
      XI*(DY*CW*CP+DZ*SW*CP))
0026      XC=CC*XT*(1.0/ZI)
0027      B(2,1)=-COZ*(ZI*CP*SK+YI*SP)
0028      B(2,2)=-COZ*(ZI*(CW*CK-SW*SP*SK)+YI*SW*CP)
0029      B(2,3)=-COZ*(ZI*(SW*CK+CW*SP*SK)-YI*CW*CP)
0030      B(2,4)=-COZ*(ZI*(-DX*CP*CK-DY*(CW*SK+SW*SP*CK)+DZ*(CW*SP*CK
      )-SW*SK)))
0031      B(2,5)=-COZ*(ZI*(DX*SP*SK-DY*SW*CP*SK+DZ*CW*CP*
      )-SK)-YI*(DX*CP+DY*SW*SP-DZ*CW*SP))
0032      B(2,6)=-COZ*(ZI*(-DY*(SW*CK+CW*SP*SK)+DZ*(CW*CK-SW*SP*SK))+
      YI*(DY*CW*CP+DZ*SW*CP))
0033      YC=CC*YT*(1.0/ZI)
0034      DO 126 I=1,3
0035      B(1,1+I)=B(1,1)
0036      B(2,1+I)=B(2,1)
0037      DO 125 I=1,2
0038      DO 125 J=1,6
0039      B(1,J)=(-1.0)*B(1,J)
0040      B(2,J)=B(2,J)
125      CONTINUE
0041      RETURN
0042      END

```


*** SAMPLE DATA BLOCK TRIANGULATION ***

-0 1.52 2	3	5			
10 00 0.0					
4					
11 55 .2 3	0.0				
9 32 .4 6	0.0				
84 .0 85	0.0				
0.00 10 9					
0.34 90 7					
1.39 62 6					
0.00 25	0.0	0.0	0.0	0.0	0.0
0.0	0.00 25	0.0	0.0	0.0	0.0
0.0	0.0	0.00 25	0.0	0.0	0.0
0.0	0.0	0.0	131.712	0.0	0.0
0.0	0.0	0.0	0.0	32.828	0.0
0.0	0.0	0.0	0.0	0.0	32.828
-27 .7 13 4	12.2 54 9				
1					
10 00 .0	0.0				
10 00 .0	0.0				
1 00 .0	0.0				
0.0	0.0	0.0			
0.0	0.0	0.0			
0.0	0.0	0.0			
6 .9 52 3	0.6 42 8				
2					
11 72 .2 3	0.0				
8 94 .4 6	0.0				
87 .4 9	0.0				
10 00 0.0	0.0	0.0			
0.0	10 00 0.	0.0			
0.0	0.0	10 00 0.0			
-0 .0 27 3	7 .4 64 3				
4					
11 29 .2 3	0.0				
9 98 .4 6	0.0				
23 .9 63	0.0				
0.0	0.0	0.0			
0.0	0.0	0.0			
0.0	0.0	0.0			
10 .8 40 2	7 .2 35 3				
5					
11 55 .2 3	0.0				
9 82 .4 6	0.0				
91 .9 67	0.0				
10 00 0.0	0.0	0.0			
0.0	10 00 0.	0.0			
0.0	0.0	10 00 0.0			

Thesis
S935

Sweet

119759

An investigation to
to improve selenodetic
control through surface
and orbital lunar
photography.

2 NOV 70

DISPLAY

Thesis
S935

Sweet

119759

An investigation to
to improve selenodetic
control through surface
and orbital lunar
photography.

thesS935

An investigation to improve selenodetic



3 2768 002 04933 0

DUDLEY KNOX LIBRARY